IDO - 14520

IDAHO CHEMICAL PROCESSING PLANT
TECHNICAL PROGRESS REPORT
January – March 1960

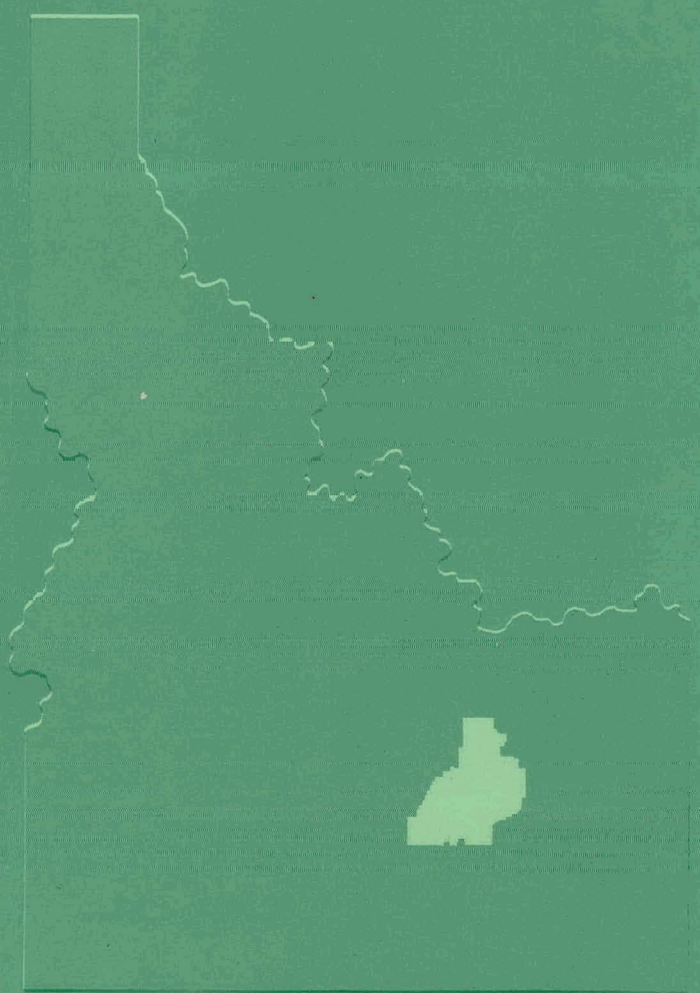

PHILLIPS PETROLEUM COMPANY

ATOMIC ENERGY DIVISION

NATIONAL REACTOR TESTING STATION

US ATOMIC ENERGY COMMISSION

DISCLAIMER

PRICE $1.50

Available from the
Office of Technical Services
U. S. Department of Commerce
Washington 25, D. C.

Printed in USA

PAGES 1 to 2

WERE INTENTIONALLY

LEFT BLANK

AEC Research and Development Report
Chemistry-Separations Processes for
Plutonium and Uranium
TID-4500, Edition-15

IDAHO CHEMICAL PROCESSING PLANT

TECHNICAL PROGRESS REPORT
JANUARY-MARCH 1960

Submitted: July 13, 1960

Issued: August 10, 1960

Submitted By: C. M. Slansky, Mgr. Chem. Dev.

F. M. Warzel, Mgr. Proc. Dev.

Edited By: J. R. Bower, Jr.

Approved By: J. A. McBride, Tech. Dir.

J. R. Huffman, Ass't. Mgr., Tech.

PHILLIPS PETROLEUM COMPANY
Atomic Energy Division
Contract AT(10-1)-205

ATOMIC ENERGY COMMISSION - IDAHO OPERATIONS OFFICE

Previous Reports in Series:

IDO-14324
IDO-14337
IDO-14350
IDO-14354
IDO-14362
IDO-14364
IDO-14383
IDO-14385
IDO-14391
IDO-14400
IDO-14410
IDO-14419
IDO-14422
IDO-14430
IDO-14443
IDO-14453
IDO-14457
IDO-14467
IDO-14471
IDO-14494
IDO-14509
IDO-14512

TABLE OF CONTENTS

LIST OF TABLES

LIST OF TABLES (Continued)

LIST OF FIGURES

THIS PAGE

WAS INTENTIONALLY

LEFT BLANK

I. SUMMARY

The ICPP processing schedule included MTR, ETR and other aluminum type fuels which were processed through the TBP headend at 75 to 100 percent of flowsheet rates and through the Hexone second and third cycle extraction system at up to 150 percent of flowsheet values achieving an over-all recovery of 99.60 percent. Stainless steel (SIR) fuel was processed through the dissolution and TBP headend extraction system at essentially full flowsheet rate with 99.69 percent recovery. Discovery that plutonium at a concentration of >1.5 μg/l is carried into the waste Amsco from the TBP scrub system has led to the suggested use of a ferrous sulfamate contactor-carbon bed absorber system for cleanup of this stream before incineration.

In carrying out basic studies on aqueous zirconium processing, results obtained during the potentiometric titration of zirconium-fluoride-nitric acid solutions with sodium hydroxide were explained by a mechanism in which the untitrated zirconium fluoride species is converted to a fluozirconate and further hydrolysis proceeds via a fluozirconate route. A modified Zirflex flowsheet for processing 2.5 percent uranium-zirconium alloy fuels is proposed as a result of bench scale dissolution studies on unirradiated PWR plates which showed that dissolver solutions could be stabilized by adding aluminum nitrate and nitric acid, that higher ammonium fluoride concentrations increased the dissolution rate, that higher hydrogen peroxide concentrations lowered the dissolution rate and decreased solution stability, and that ammonia removal by boiling with or without air sparging had little effect on the reaction. Density curves for Zirflex solutions are reported.

First tests of the pilot plant for continuous dissolution of zirconium type elements have indicated that the dissolution rate is approximately four times as great as predicted on the basis of batch dissolution rates and comparison with the rate ratio for batch vs continuous dissolution of aluminum which was used to establish the dissolver size. The continuous dissolution rate for a two percent zirconium-98 percent uranium element was approximately proportional to the acid feed rate and reached 190 kg/day at an acid feed rate of 36 liters/hour (11M nitric acid, 0.30M hydrofluoric acid, 0.35M aluminum nitrate).

Development of new waste treatment methods is influenced by waste volumes and the associated storage costs involved. A survey of current and proposed zirconium fuel processes indicates highest waste volumes are generated by the Zirflex and the original STR processes, with moderate improvement for the currently modified STR process. An approximate order of magnitude reduction is indicated for headend treatment with Ba^{++} to precipitate barium fluozirconate and even greater reduction is promised by the ARCO process. The possibility of separation of at least 98 percent of the base alloy components from acidic, stainless steel waste solutions is indicated by polarographic study which demonstrated that iron, chromium and nickel reduction by mercury cathode electrolysis can proceed without reduction of cesium-137, cerium-144 and strontium-90, as long as the total electrolyte concentration is maintained at or above 0.02M. Preliminary work on the calcination of aqueous zirconium wastes, using calcium oxide

as a precipitant prior to calcination and silica as a scavenger in the calciner, indicate that retention of the fluoride will be difficult. Continued study on removal of cesium-137 from process waste solutions by ammonium phosphomolybdate indicates the APM to have high affinity for cesium in acid solutions and in the presence of aluminum nitrate, and to have reasonable stability in mineral acids, other than hydrofluoric acid, up to 1.0N acid.

In identification of ionic species present in process solutions, electrolytic conductance has been useful as an analytical tool; data obtained are of significance in application to process problems as well as instrumental analysis and control. The Onsager-Fuoss limiting law for electrical conductance of electrolyte mixtures has been tested by measurements of KCl-HCl mixtures at 25°C and, within experimental error, has been confirmed.

Experiments on electrolytic dissolution of stainless steel in nitric acid, designed to study the quantity of anode sludge formed as the temperature was varied from 40°C to 90°C, the current density from 0.4 to 1.2 amp/cm^2, and the acidity from 1M to 5M, disclosed that minimum sludge (0.2 to 0.5 grams/100 grams of metal dissolved) was formed at the lower temperature and under high current density-high acidity or low current density-low acidity conditions. Other combinations of these variables gave 1 to 3 grams of sludge per 100 grams of metal dissolved. Acidity, or the combination of hydrogen ion and nitrate ion, was the only variable affecting stoichiometry of the reaction, with 1.33 and 1.45 moles of nitric acid being consumed per equivalent of metal dissolved at 1M and 5M hydrogen ion concentration, respectively. Separation of stainless steel cladding from a uranium dioxide core by means of electrolytic dissolution appears possible as a result of data showing uranium losses to the dissolver solution as low as 0.3 to 0.4 percent for ten minutes contact at 13°C. Potential vs current density data show that stirring the electrolyte solution increases the limiting current density by a factor of 2.5.

An extension of the ARCO process, which employs molten lead chloride as a solvent for zirconium-uranium alloys followed by regeneration of lead chloride from the lead produced, utilizes direct chlorination in the dissolver vessel to rechlorinate lead as it is formed, or to directly chlorinate (by addition of chlorine to the lead chloride bath) and rapidly dissolve a wide variety of metals including stainless steel, chromium, niobium, aluminum and zirconium at rates of at least 15 to 30 mg/cm^2/minute. Relatively rapid attack eliminates many materials from consideration for dissolver construction but an alumina ceramic appeared to withstand the dissolution medium.

In continued studies of solvent stability in the TBP-HNO_3-zirconium system, it has been shown that (1) the zirconium-TBP reaction is first order with respect to zirconium concentration, (2) the half time for the reaction increases as the zirconium concentration increases, and (3) the activation energy is 21.0 kilocalories. At 50°C the half time of the reaction is about 15 hours.

II. ICPP OPERATIONAL SCHEDULE, PERFORMANCE AND PROBLEMS

A. ICPP Processing Schedule, J. R. Bower

The processing of MTR, ETR and other miscellaneous aluminum fuels started last quarter was completed this period with over-all recovery of 99.60 percent. Stainless steel (SIR) fuel was processed through the dissolution and TBP headend extraction system with 99.69 percent recovery. This headend product was stored, pending completion of zirconium (STR) headend processing which was started at the end of the period. These two materials (SIR and STR) will be blended and processed together through the second and third Hexone cycles for final cleanup.

Table 1 shows quantities of material dissolved and the schedule followed in ICPP operations during this quarter.

Table 1

DISSOLUTION SCHEDULE AT ICPP, JANUARY-MARCH, 1960

Week Ending	MTR Elements Kg.U	MTR Elements No.	ETR Elements Kg.U	ETR Elements No.	Other Aluminum Elements	SIR Elements	STR Elements
Jan. 2	6.9	46	47.1	184	X		
Jan. 9*							
Jan. 16			8.0	40	X		
Jan. 23					X		
Jan. 30			17.6	80	X		
Feb. 6*					X		
Feb. 13*						X	
Feb. 20*						X	
Feb. 27						X	
Mar. 5						X	
Mar. 12						X	
Mar. 19							X
Mar. 26							X

*Second and third cycle (Hexone) system operating

Three barium-140 runs were completed with no unusual difficulties or problems. The product recovery was as listed in Table 2.

Table 2

BARIUM-140 PRODUCTION AT ICPP, JANUARY-MARCH, 1960

Run No.	Curies	Percent Recovery
038	31,760	58.3
039	20,000	41.0
040	31,200	56.6

B. MTR-ETR and Miscellaneous Aluminum Alloy Fuel Processing,
J. R. Bower, Problem Leader; G. J. Raab

The processing of MTR, ETR and other miscellaneous aluminum fuels started last quarter was completed this period with over-all recovery of 99.60 percent. The flowsheet for the run was presented in the preceding quarterly report.(1)

The mode of operation was different from previous runs in that, because of a limited operating crew, the first cycle product was held up in storage banks before being sent into the second and third cycles. The same crew alternately worked the dissolution and first cycle system, and the second and third cycle system as required. This mode of operation resulted in two CPM (first cycle) and two second and third cycle operating periods.

1. Operating Observations

The first cycle operation resulted in an average processing rate equal to 75 percent of the flowsheet value. There were periods of satisfactory 100 percent flowsheet operation; however, recycle of raffinate and feed control problems limited the rate at other times. Column operation was smoother (minimum of column upsets) than when processing high silica fuels; the need for recycle of waste batches resulted from either off-specification feed or pulser troubles. Off-specification feed occasionally resulted from charging of unirradiated damaged ETR elements with the irradiated fuel and the resulting difficulty in controlling catalyst addition and dissolution rate in the continuous dissolver.

It appears desirable to schedule fuel dissolution to avoid mixing materials with widely differing dissolving characteristics, in the interest of maintaining uniform column feed.

Second and third cycle operations were of quite short duration because, after getting the systems lined out, it was possible to process out of first cycle product storage at rates equal to 150 percent of flowsheet. Over-all performance of the run was good. The waste loss from first cycle was 0.39 percent and from second and third cycles 0.013 percent.

Exact decontamination performance was obscured by the fact that the feed varied (a mixture of fuels, plus irradiated and unirradiated fuels) and the first cycle product was stored before processing through second and third cycles. Table 3 presents some typical radiochemical analyses for the run. The fresh feed and IDP data represent results at one operating period, and the IIAF, IIBP and IIIBP data represent results at another operating period. Thus the results are not directly comparable. Operation and decontamination have in general been so satisfactory that the taking of a larger number of samples for purely informational purposes has not been felt justified.

Table 3

DECONTAMINATION RESULTS OF PROCESSING ALUMINUM ALLOY FUELS
(TBP First Cycle, Hexone Second and Third Cycles)
Activity in d/(min)(g.U)

	Total Beta Activity	Total Gamma Activity	Ruthenium	Niobium	Zirconium
Fresh Feed	3.28×10^{13}	2.12×10^{13}	4.77×10^{11}	5.37×10^{10}	7.33×10^{11}
IDP	2.72×10^{10}	4.94×10^{10}	1.30×10^{9}	2.87×10^{9}	7.76×10^{9}
IIAF*	8.02×10^{8}	4.13×10^{9}	2.00×10^{8}	9.34×10^{7}	1.53×10^{9}
IIBP	1.40×10^{7}	6.25×10^{7}	3.06×10^{6}	3.14×10^{7}	1.41×10^{7}
IIIBP	1.30×10^{7}	2.21×10^{7}	3.48×10^{5}	7.23×10^{4}	1.70×10^{5}
First Cycle DF	1210	432	367	18	94
Over-All DF	2.56×10^{6}	9.60×10^{5}	1.37×10^{6}	7.45×10^{5}	4.32×10^{6}

*IIAF calculated from a IIAR sample since the IIAF is not directly sampled

C. Stainless Steel (SIR) Processing, J. R. Bower, Problem Leader; G. J. Raab

Stainless steel (SIR) fuel was processed through dissolution and first cycle TBP extraction this quarter with 99.69 percent recovery using the flowsheet published in the second preceding quarterly report[2] of this series. The product from the run was stored in cell B and will be combined with STR (zirconium) fuel product for processing through the Hexone second and third cycles.

The IA column loss (extraction), based on raffinate discharged to waste, was 0.18 percent. The IB column loss (scrub), on a like basis, was 0.02 percent. The remaining loss of 0.11 percent was attributable to the IC column (strip). However, had not the majority of the ISW (first solvent recovery mixer settler effluent) been recycled the loss due to the strip column would have been at least one percent.

1. Operating Observations

The dissolver operation gave difficulty early in the run when two batches failed to initiate, presumably due to nitrate ion-induced passivation. Procedure revision to assure draining and rinsing of jet and instrument dip tubes in the dissolver, to eliminate holdover of dissolver acids from a preceding batch, apparently solved the problem. The average dissolution cycle after elimination of this difficulty was 8.5 hours with an average of 9.7 batches between heel cleanouts.

The IA column performed well except when the pulser lost its charge. It was necessary to check the pulsers frequently. Two batches of raffinate were reworked to recover approximately 150 grams of uranium, or about as much uranium as was discharged to waste during the rest of the entire run from all sources.

The IC column (stripping) performance was poor during most of the run with the solvent recovery wash (first stage) picking up sufficient uranium to require recycling to the extraction chain. After five days of poor recovery at a flowsheet ratio of one part aqueous to four parts organic, the aqueous flow was raised to give a ratio of one to three. This failed to improve the stripping obtained. The solvent in the system was then changed since the original solvent had been saved from a previous stainless steel run four months earlier. This, likewise, did not improve the stripping obtained in the IC column. The ammonia concentration of the IBS (scrub) stream was found to be somewhat below the flowsheet requirement, possibly resulting in excess acid in the IBP (C column feed) stream, and adjustment of this improved the stripping obtained although recycle of the solvent wash was still required to recover unstripped uranium. During all of this period the column pulser was the object of considerable attention, receiving numerous adjustments and rechargings, with some indication that it was not holding its charge (air was usually bled off the system) and thus not imparting sufficient energy to the column. Near the end of the run operation improved and it was possible to dispose of a number of batches of solvent wash without first recovering uranium.

Decontamination across the first cycle was good. Table 4 shows the decontamination results for the run.

Table 4

DECONTAMINATION RESULTS OF PROCESSING STAINLESS STEEL (SIR) FUEL
(First Cycle TBP System)
Activity in d/(min)(g.U)

	Total Beta Activity	Total Gamma Activity	Ruthenium	Niobium	Zirconium
Fresh Feed	9.15×10^{12}	3.05×10^{12}	1.12×10^{11}	2.80×10^{11}	1.49×10^{11}
IDP	1.02×10^{9}	1.21×10^{9}	2.35×10^{8}	5.17×10^{7}	3.21×10^{7}
DF	8.97×10^{3}	2.52×10^{3}	4.77×10^{2}	5.42×10^{3}	4.64×10^{3}

D. Plutonium Contamination of Solvent, J. R. Bower, Problem Leader; P. N. Kelly

An experimental program was undertaken this period to determine the level of plutonium contamination in waste Amsco from the ID scrub column of the TBP system and to test a carbon absorber for cleanup of the stream. Maximum permissible plutonium in this waste stream, which is disposed of by burning, was recently established as 1.5 μg/l by the IDO Health and

Safety Division after discovery of waste Amsco containing up to 400 ug/l of plutonium.

Prior to this discovery waste Amsco had never been analysed for plutonium; the routine analyses before transfer for disposal had been for uranium and gross activities. When first noted, the high plutonium was believed to have resulted from the transfer of TBP-Amsco solvent to the system during plant cleanout and a temporary procedure for scrubbing the Amsco with ferrous sulfamate solution in existing equipment was developed. The procedure, while crude, was successful in reducing plutonium to safe disposal levels.(2) Since, however, routine sampling has revealed that the waste Amsco stream, when processing aluminum-type fuels, normally averages above 1.5 µg/l and a permanent cleanup procedure must be considered.

1. Plutonium Distribution Study

Because solubility considerations indicated that plutonium should be several orders of magnitude below 1.5 µg/l in the Amsco stream, an investigation was made to adequately define the behavior of plutonium in the process. Flowing stream samples were taken during CPM processing (aluminum-type fuels) and plutonium concentrations in process streams and a material balance are given in Table 5.

Table 5

PLUTONIUM BALANCE IN TBP FIRST CYCLE EXTRACTION SYSTEM

Stream	IAF	IAR	ICR	IDP	IDR	Balance
Plutonium (µg/l)	442	43.4	10.6	646	9	
Plutonium (percent)	100	10.2	1.9	61.0	0.05	73.1

In an attempt to reduce plutonium in the D column, and thence in the waste Amsco, ferrous sulfamate was added to the IA feed, the ferrous ion to reduce plutonium to the non-extractable plus III valence state and the sulfamate to stabilize it in that state by removing nitrous acid present in the feed. With a IA feed concentration of 0.01M ferrous sulfamate the plutonium in the ID column decreased from 61 percent to 3 percent of that in the feed, the bulk of the plutonium being diverted to the A column raffinate. Plutonium, however, persisted essentially unchanged in concentration in the waste Amsco stream. Microgram quantities of plutonium apparently complex, either as a plutonium polymer or a mono- or di-butyl phosphate compound, and carry through the process to the D column organic.

2. Carbon Absorber Test

Concurrent with the ferrous sulfamate test, experimental equipment was set up to determine the capacity of activated carbon for absorbing plutonium from the waste Amsco stream. Laboratory scoping studies had indicated that some of the plutonium was compounding into a species which would not scrub into a ferrous sulfamate solution but which would readily absorb on a variety of surfaces. The affinity of this

species for activated carbon had been established, but a plant scale test was needed to obtain absorption capacity.

For the experiments, Amsco from the waste collection tank was recirculated through a 1-inch diameter by 12-inch long carbon bed at a rate to provide a three minute residence time. A capacity of at least 16,000 $\mu g/ft^3$ was obtained. This figure may be small because breakthrough occurred during circulation of a batch of Amsco which had been contacted with decontaminating chemicals and contained a large portion of relatively non-absorbable ionic plutonium, thus masking any additional plutonium absorbed during circulation of this Amsco.

3. Conclusions

It is apparent from these experiments that:

(a) Addition of ferrous sulfamate in the IA column is inadequate to reduce plutonium in the ID waste below tolerance.

(b) Carbon beds, even in conjunction with ferrous sulfamate addition in the IA column, are inadequate because of the possible presence of ionic plutonium in the waste Amsco stream, especially during decontamination operation.

(c) A feasible plutonium decontamination system for the waste Amsco stream would be a ferrous sulfamate contactor to remove ionic plutonium followed by a carbon bed to remove non-ionic plutonium.

III. AQUEOUS PROCESSING STUDIES

Section Chiefs: H. T. Hahn, Chemical Research; K. L. Rohde, Process Chemistry; J. A. Buckham, Technical Projects

The existing hydrofluoric acid dissolution process (STR) for uranium-zirconium fuels has several major disadvantages: high specific waste volumes; restriction to 1 1/2 percent or lower uranium alloys by solubility; inability to handle oxide fuels; and the liberation of hydrogen in the off-gas. New process approaches involve the measurement of certain basic properties of zirconium systems and the application of the data to flowsheet development. Aqueous systems studies are described in this section and the fused lead chloride process in Section VII.

Solubility data are necessary in the choice of dissolvent systems and for setting specifications for the permanent storage of waste solutions. Phase studies on zirconium-nitrate-fluoride solutions have been necessary because of lack of literature data. Knowledge of the species of zirconium in solution is needed to give an understanding of the reactions in solution and their behavior in chemical operations in order to establish optimum flowsheet conditions. A potentiometric titration by NaOH of the system: $Zr\text{-}NO_3\text{-}F$ is described, and the complex equilibria are explained by a fluozirconate mechanism.

The Zirflex process for zirconium fuels uses 6M NH_4F as a dissolvent and has been proposed by GE HAPO and ORNL for the zirconium decladding of UO_2 fuel. ICPP studies have modified the Zirflex process to accommodate uranium-zirconium alloys in the 2-3 percent uranium range where the original STR process is not applicable. Oxidants such as hydrogen peroxide and ammonium nitrate are added to the dissolvent to solubilize the uranium. Bench scale continuous dissolution studies on unirradiated PWR plates show that solids formed during dissolution can be solubilized by adding aluminum nitrate and nitric acid, that higher ammonium fluoride concentrations increase the dissolution rate, that higher hydrogen peroxide concentrations lower the dissolution rate and decrease solution stability, and that ammonia removal by boiling, with or without air sparging, has little effect on the reaction. From these studies a flowsheet was proposed for 2.5 percent uranium-zirconium alloy fuels for further evaluation in the pilot plant.

The density of Zirflex solutions is being determined as part of the flowsheet development program and results obtained to date are reported. These will be important in setting operation flowsheet specifications and in development of in-line control instrumentation.

The zirconium pilot plant facilities have undergone initial testing and certain deficiencies are being corrected. The dissolution rate for a 2 percent zirconium-98 percent uranium element in a nitric acid-hydrofluoric acid-aluminum nitrate solution was approximately four times as great as predicted on the basis of batch dissolution rates and of comparison with the rate ratio for batch *vs* continuous dissolution of aluminum.

A. Aqueous Zirconium Fuel Processing

1. Zirconium Phase Studies - Potentiometric Behavior of Zirconium in Nitrate and/or Fluoride Systems, E. M. Vander Wall, Problem Leader; A. J. Moffat

Study of the species present in zirconium process solutions has continued. The potentiometric behavior of zirconium-nitrate-fluoride solutions at fluoride to zirconium (F/Zr) mole ratios less than 7 can be interpreted with the aid of recent work[3] at ICPP on sodium fluozirconate phase relationships.

At low $H^{\oplus}$/Zr mole ratios (which are achieved during the titration of zirconium-nitrate-fluoride systems with sodium hydroxide) and as the F/Zr mole ratio is successively increased, the following equilibria have been suggested:[3]

$$2n\ ZrOF^{\oplus} + 2n\ OH^{\ominus} \rightleftharpoons \left[\begin{matrix} F & F \\ -Zr-O-Zr-O- \\ OH & OH \end{matrix}\right]_n \qquad (1)$$

$$\left[\begin{matrix} F & F \\ -Zr-O-Zr-O- \\ OH & OH \end{matrix}\right]_n + nF^{\ominus} \rightleftharpoons \left[\begin{matrix} F & F \\ -Zr-O-Zr-O- \\ F & OH \end{matrix}\right]_n + nOH^{\ominus} \qquad (2)$$

$$\left[\begin{matrix} F & F \\ -Zr-O-Zr-O- \\ F & OH \end{matrix}\right]_n + nF^{\ominus} \rightleftharpoons \underbrace{\left[\begin{matrix} F & F \\ -Zr-O-Zr-O- \\ F & F \end{matrix}\right]_n}_{(ZrOF_2 \cdot 2H_2O)} + nOH^{\ominus} \qquad (3)$$

$$\left[ZrOF_2\right]_s + 2H^{\oplus} + 2Na^{\oplus} + 4F^{\ominus} \rightleftharpoons \left[2NaF \cdot ZrF_4\right]_s + H_2O \qquad (4)$$

At F/Zr ratios of one (Figure 1) approximately 75 percent of the zirconium is titrated with base. These data are consistent with the formation of a zirconium monofluoride. When the F/Zr mole ratio is two, only 50 to 75 percent of the zirconium is titrated with base at the break in the titration curve. The bases for the inflection (Figure 1) are given in Equations (2) and (3). At F/Zr mole ratios ranging from three to six it is known that the zirconyl difluoride ($ZrOF_2 \cdot 2H_2O$) species and sodium hexafluozirconate are in equilibrium as described by equation (4). In this range (F/Zr $\sim$ 3 to 6) part of the zirconium is present as $2NaF \cdot ZrF_4$ and as the titrated proceeds, the $2NaF \cdot ZrF_4$ is converted to $ZrOF_2 \cdot 2H_2O$.

$$\left[2NaF \cdot ZrF_4\right]_s + 2OH^{\ominus} \rightleftharpoons \left[ZrOF_2\right]_s + 4F^{\ominus} + 2Na^{\oplus} + H_2O \qquad (5)$$

The further addition of $OH^{\ominus}$ results in the following sequence of reactions:

$$\left[ZrOF_2\right]_s \underset{F^{\ominus}}{\overset{OH^{\ominus}}{\rightleftharpoons}} \left[ZrOF(OH)\right]_s \underset{F^{\ominus}}{\overset{OH^{\ominus}}{\rightleftharpoons}} \left[ZrO(OH)_2\right]_s \qquad (6)$$

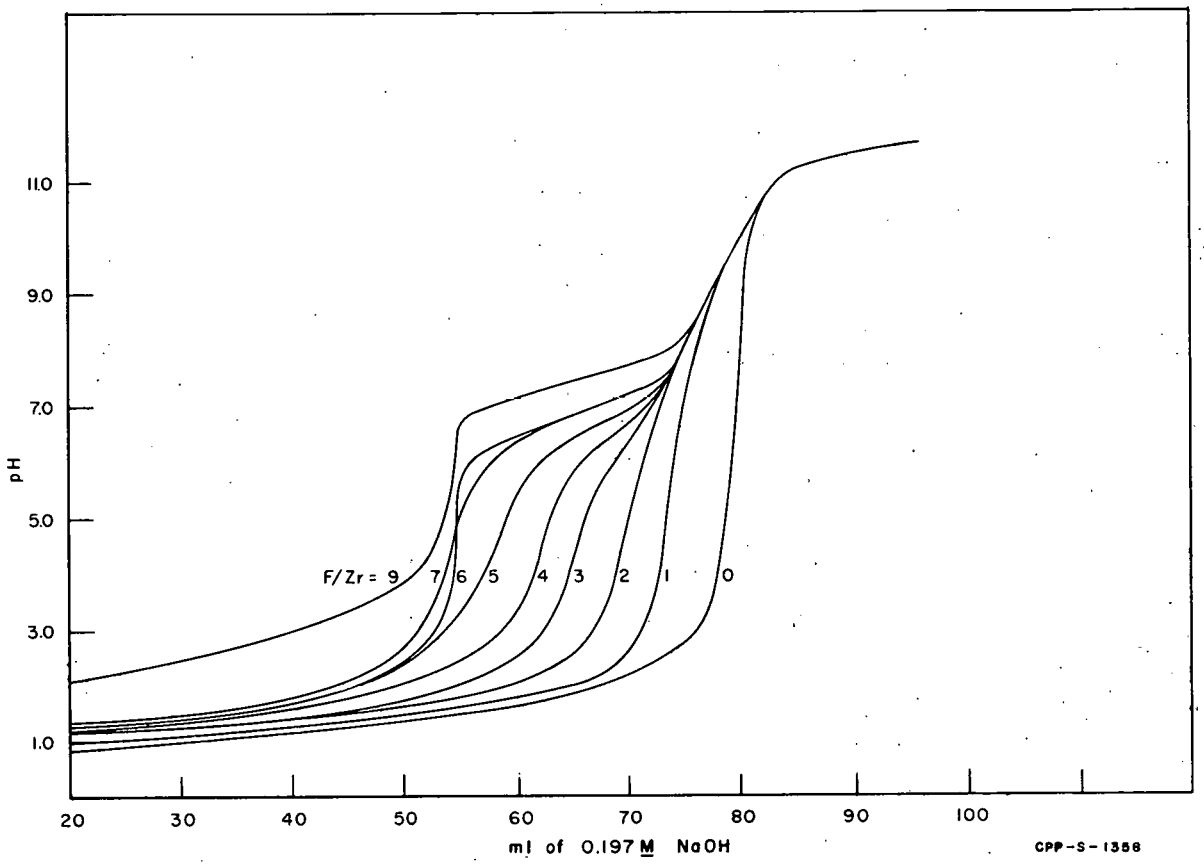

Fig. 1 - Potentiometric Titration of Zirconium-Fluoride-Nitric Acid Solutions at Various F/Zr Mole Ratios (2.0 ml sample; 0.61M Zr-7.83M $NO_3^{\ominus}$)

Equations (5) and (6) are derived from sodium fluozirconate phase studies carried out in this laboratory.(3) At a F/Zr ratio of seven the general hydrolysis reaction would likely be:

$$\left[3NaF \cdot ZrF_4\right]_s + 2OH^{\ominus} \rightleftharpoons \left[ZrOF_2\right]_s + 3Na^{\oplus} + 5F^{\ominus} + H_2O \qquad (7)$$

followed by the reaction described by equation (6).

The general conclusions which can be drawn at this time are that as zirconium-fluoride systems are titrated with base, with liberation of fluoride, the untitrated zirconium fluoride species is converted to a fluozirconate and further hydrolysis proceeds via a fluozirconate mechanism.

2. Homogeneous Continuous Dissolution of 2.5 Percent Uranium-Zirconium Alloys Using the Zirflex Process, K. L. Rohde, Problem Leader; B. J. Newby and C. E. May

The homogeneous dissolution of uranium-Zircaloy-2 alloy in ammonium fluoride solution with an added oxidant has been studied in a bench scale

continuous dissolver. A continuous dissolution flowsheet is presented and recommended for pilot plant testing.

Previous batch dissolution work[2] indicated that either ammonium nitrate or hydrogen peroxide might be effective oxidants to be used in conjunction with ammonium fluoride for homogeneous dissolutions. Later work[1], involving dissolution of uranium-Zircaloy-2 alloys in ammonium fluoride-hydrogen peroxide, pointed out some of the variables that should be scoped in a continuous dissolution study. In the present study homogeneous continuous dissolution of the alloys was achieved by the use of ammonium fluoride and either ammonium nitrate or hydrogen peroxide but the resulting dissolver solution was unstable at room temperature. The dissolver solution could be stabilized by the addition of aluminum nitrate and nitric acid while holding the solution at a temperature of 50°C during the additions.

a. Experimental Equipment and Procedure

All studies were carried out in the stainless steel continuous dissolver depicted in Figure 2. The vertical portion of the dissolver consisted of a 1-1/2 inch (schedule 40) pipe closed at the bottom end by a pipe cap; the fuel chute, feed inlet lines, and dissolver solution outlet lines were constructed of various sizes of stainless tubing as indicated. Heat was supplied by heating tape wrapped around the dissolver between the lower liquid feed inlet and the dissolver solution outlet. A perforated stainless steel plate located just above the point where the fuel chute is attached to the dissolver, kept large particles within the lower portion of the dissolver. A piece of tygon tubing attached to the end of the dissolver solution outlet was bent upward sufficiently to keep the liquid level in the vertical portion of the dissolver above the outlet. This prevented dilution of the dissolver solution in the outlet with vapor. Liquids were fed into the dissolver by means of Sigmamotor pumps. In runs involving air sparging, air was metered into the dissolver through a glass tube located in the fuel chute and extending into the vertical portion of the dissolver. During runs in which vapor was allowed to escape from the dissolver without reflux (the vapor loss being replaced by water addition to the dissolver), and during boil-up measurements at the end of a run carried out under total reflux, the condenser and thermometer shown in Figure 2 were replaced by a connecting tube which collected vapor from the dissolver, directing it out of the dissolver and downward through a water cooled condenser.

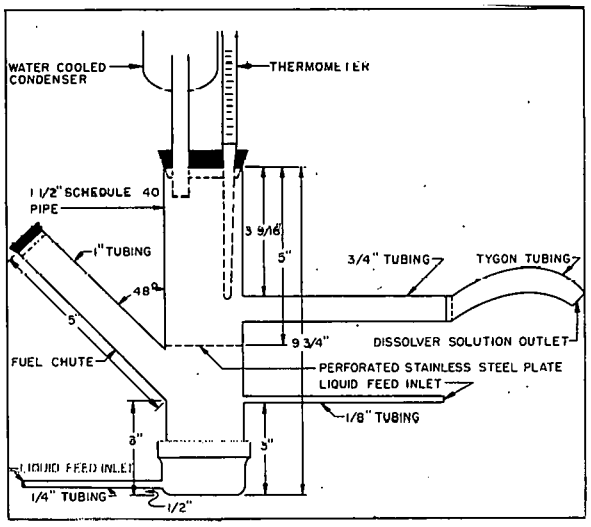

Fig. 2 - Laboratory Model of Zirflex Continuous Dissolver

All dissolutions were carried out using 295 ml of solution, at the boiling point of that solution. About 40 grams (0.37 cubic inches) of undissolved uranium-Zircaloy-2 alloy were present in the dissolver during the run. The 2.5 percent uranium segments used were cut from PWR type fuel plates which consisted of Zircaloy-2 cladding and 5.83 percent by weight normal uranium plus Zircaloy-2 filler. Plate rolling temperature was 1450°F with a preheat time of 75 minutes and post heat time of 15 minutes.

The dissolution was considered to be at equilibrium if the zirconium and uranium concentrations (as indicated by "on the spot" colormetric analysis) of the dissolver effluent remained constant for 3 hours. After dissolver equilibrium had been established, dissolver effluent was directed into a settling container held at 50°C; portions of the clarified effluent from the upper portion of the settling vessel were either stabilized with nitric acid and aluminum nitrate (to be used for zirconium, uranium, and fluorine analysis) or allowed to stand overnight for short term stability studies.

b. Observations

The continuous homogeneous dissolution of uranium-Zircaloy-2 alloy in ammonium fluoride-hydrogen peroxide (or ammonium nitrate) was studied as a function of liquid feed rate, ammonium fluoride concentration, oxidant concentration, ammonia removal techniques, liquid feed introduction techniques, and boil-up. Since it became apparent early in these studies that the dissolver solution produced during the dissolution of the alloy in ammonium fluoride-hydrogen peroxide (or ammonium nitrate) would be unstable at room temperature, methods for stabilizing this solution were investigated.

(1) Liquid Feed Rate

Other conditions being constant, an increase in liquid feed rate gives a higher dissolution rate, although decreasing the zirconium concentration of the dissolver effluent. This results in a higher effluent pH. However, as shown in Table 6, liquid feed rate has little effect on the percentage of alloy uranium dissolved as compared with 100 percent dissolution of zirconium. X-ray examination of the solids separating from the dissolver effluent after aging indicates the major component to be $(NH_4)_3ZrF_7$.

(2) Ammonium Fluoride Concentration

Increasing the ammonium fluoride concentration in the dissolver feed stream, under the conditions summarized in Table 7, increased the dissolution rate sufficiently to lower the fluoride-zirconium mole ratio of the product to a value which resulted in stable dissolver effluent in batch dissolution work. The first two runs in Table 7, using the higher ammonium fluoride concentrations, did not come to equilibrium conditions due to localized solid formation (identified primarily as $(NH_4)_3ZrF_7$) within the dissolver. This solid formation can be prevented by air sparging. Higher ammonium fluoride feed concentrations also resulted in increased uranium dissolution.

Table 6

DISSOLUTION OF URANIUM-ZIRCALOY-2 ALLOY
EFFECT OF LIQUID FEED RATE

Conditions: Total reflux; Liquid feed composition, 5.1M NH_4F-0.065M H_2O_2; Boil-up, 2 ml/min.

Liquid Feed Rate	Dissolution Rate	Effluent Composition				Completeness of Uranium Dissol.(a)	Solids in Aged Effluent(b)
		Zr	U	F/Zr	pH		
ml/min	mg/(cm^2)(min)	M	g/l	Mole Ratio		Percent	g/l
3.3	5.6	0.50	0.69	9.9	8.2	58	89
1.9	2.3	0.77	0.88	8.4	7.3	48	98

(a) Proportional uranium dissolution as compared with zirconium dissolution (100 percent would indicate equivalent uranium to zirconium dissolution for 96 percent zirconium-2.5 percent uranium fuel).
(b) Solids formed on standing overnight.

Table 7

DISSOLUTION OF URANIUM-ZIRCALOY-2 ALLOY
EFFECT OF AMMONIUM FLUORIDE CONCENTRATION

Conditions: Total reflux; Liquid feed rate, 2.6 ml/min; Boil-up, 5.5 ml/min; Oxidant, 0.065M H_2O_2 in NH_4F

Ammonium Fluoride	Dissolution Rate	Effluent Composition				Completeness of Uranium Dissolution	Solids in Aged Effluent
		Zr	U	F/Zr	pH		
M	mg/(cm^2)(min)	M	g/l	Mole Ratio		Percent	g/l
6.0	5.7	0.68(a)		6.8(a)			
5.1	4.4	0.57	0.9	8.0	7.3	67	47
4.7	3.6	0.57	0.53	7.7	7.3	39	33

(a) Calculated from volume of feed and weight of fuel dissolved, assuming the fuel to be 96 percent zirconium. Sample not analyzed because of excessive solids.

(3) Hydrogen Peroxide Concentration

In the runs summarized in Table 8, increasing the hydrogen peroxide concentration in the dissolver feed did not markedly increase the extent of uranium dissolution, but did decrease the dissolution rate sufficiently to prevent solid formation within the dissolver.

Table 8

DISSOLUTION OF URANIUM-ZIRCALOY-2 ALLOY
EFFECT OF HYDROGEN PEROXIDE CONCENTRATION

Conditions: Total reflux; Liquid feed rate, 2.6 ml/min; Boilup, 5.5 ml/min.

Liquid Feed Composition	Dissolution Rate	Effluent Composition				Completeness of Uranium Dissolution	Solids in Aged Effluent
		Zr	U	F/Zr	pH		
	mg/(cm^2)(min)	M	g/l	Mole Ratio		Percent	g/l
5.1M NH_4F 0.065M H_2O_2	4.4	0.57	0.9	8.0	7.3	67	47
5.1M NH_4F 0.3M H_2O_2	3.9	0.63	1.1	8.2	7.5	74	85

(4) Ammonia Removal Techniques

Initially it was thought that more effective ammonia removal during dissolution would result in more stable dissolver effluents. Ammonia removal was attempted by allowing vapor produced during a dissolution to escape from the dissolver, unrestricted, and replacing the vapor loss with water. The results of such a run are compared in Table 9 with a run made under total reflux. The effluent pH indicates that ammonia removal was not increased by this technique. However, the dissolution rate was decreased, the fluoride to zirconium mole ratio was increased, and the uranium dissolution improved.

An attempt was also made to increase ammonia removal by air sparging (see Table 9). The only apparent effect of air sparging was to keep the solution within the dissolver stirred sufficiently to prevent solid formation caused by local action.

(5) Boil-up

Boil-up, over the range shown in Table 10, had no noticeable effect on dissolutions carried out without reflux. Water, to replace the vapor loss, was added to the dissolver through the upper liquid feed inlet (see Figure 2). Complete uranium dissolution was realized in these runs.

In dissolutions carried out under total reflux, an increase in boil-up increased the dissolution rate and decreased the fluoride-zirconium mole ratio. Although no two total reflux dissolutions were performed in which boil-up was the only variable, dissolution runs were made differing only in boil-up and liquid feed rate. Comparing the results of the second run tabulated in Table 7, with the two summarized in Table 6, leads to the conclusion that the increase in boil-up from 2.0 to 5.5 ml/min under total reflux resulted in a decrease in the fluoride-

zirconium mole ratio and, possibly, a slight increase in zirconium dissolution rate.

Table 9

DISSOLUTION OF URANIUM-ZIRCALOY-2 ALLOY
EFFECT OF AMMONIA REMOVAL TECHNIQUES

Conditions: NH_4F-H_2O_2 feed rate, 2.6 ml/min; Concentration, 5.1M NH_4F-0.065M H_2O_2; Boil-up, 5.5 ml/min.

Ammonia Removal Technique	Dissolution Rate	Effluent Composition				Completeness of Uranium Dissolution	Solids in Aged Effluent
		Zr	U	F/Zr	pH		
	mg/(cm²)(min)	M	g/l	Mole Ratio		Percent	g/l
Vapor allowed to escape unrefluxed, loss replaced by water	3.0	0.57	1.5	9.7	8.4	>90	89
None, total reflux	4.4	0.57	0.9	8.0	7.3	67	47
Total reflux, sparging with 7 l/min of air (at 14.7 psi and 70°F)	4.5	0.63	0.8	7.9	7.4	53	77

Table 10

DISSOLUTION OF URANIUM-ZIRCALOY-2 ALLOY
EFFECT OF BOIL-UP

Conditions: Dissolution without reflux, replacing vapor loss with water; Liquid feed composition, 5.1M NH_4F-0.065M H_2O_2; Liquid feed rate, 2.6 ml/min.

Boil-up	Dissolution Rate	Effluent Composition				Completeness of Uranium Dissolution	Solids in Aged Effluent
		Zr	U	F/Zr	pH		
ml/min	mg/(cm²)(min)	M	g/l	Mole Ratio		Percent	g/l
1.6	3.4	0.57	1.6	9.7	8.2	>90	89
4.5	3.0	0.57	1.5	9.7	8.4	>90	89

(6) Dissolver Solution Stability

Three dissolution experiments were directed at stabilization of a dissolver effluent by achieving a low fluoride-zirconium mole ratio. In the first run, the objective was to increase the zirconium dissolution rate faster than the fluoride feed rate by using a high boil-up and high ammonium fluoride concentration under total reflux; to realize high uranium dissolution, a 1M hydrogen peroxide feed stream was used in the upper feed line. Air sparging was used to prevent solid formation and to minimize contact of the undissolved alloy with hydrogen peroxide. The higher fluoride-zirconium mole ratio actually realized in this run (see Table 11) was apparently brought about by the higher hydrogen peroxide concentration, decreasing the zirconium dissolution rate even in the presence of air sparging.

Table 11

DISSOLUTION OF URANIUM-ZIRCALOY-2 ALLOY
DISSOLUTIONS ATTEMPTING DISSOLVER EFFLUENT STABILIZATION

Conditions: Total reflux; Boil-up, 5.5 ml/min; Sparging with 7 l of air/min (measured at 14.7 psia at 70°F).

Liquid Feed Composition and Rate		Dissolution Rate	Effluent Composition				Completeness of Uranium Dissolution	Solids in Aged Effluent
			Zr	U	F/Zr	pH		
Upper Stream	Lower Stream	mg/(cm²)(min)	M	g/l	Mole Ratio		Percent	g/l
1M H_2O_2 at 0.6 ml/min	6.0M NH_4F at 2.6 ml/min	4.2	0.58	1.2	9.2	8.3	88	79
0.5M H_2O_2 at 0.5 ml/min	5.1M NH_4F at 1.8 ml/min	2.4	0.55	0.35	7.5	7.6	27	4
Water at 0.6 ml/min	6.0M NH_4F-1M NH_4NO_3 at 2.6 ml/min	5.8	0.65	1.6	7.6	7.7	>90	96

A lower fluoride-zirconium mole ratio, resulting in increased effluent stability, was realized in the second run. This was accomplished by using a lower hydrogen peroxide concentration in the feed stream entering the dissolver above the alloy and by allowing more contact time between ammonium fluoride and the alloy. Uranium dissolution, however, was unsatisfactory.

Complete uranium dissolution and a low fluoride-zirconium ratio were achieved in the third run, again utilizing two feed streams; the lower stream was ammonium fluoride-ammonium nitrate and the upper one was water. The dissolver effluent, however, was not stable.

Unsuccessful attempts were made to stabilize the solution overflowing from the dissolver by adding nitric acid, adding hydrogen peroxide, diluting with water, and adding water plus nitric acid. Successful effluent stabilization was obtained by following an ORNL flowsheet[4] which involved the addition of aluminum nitrate and nitric acid while holding the solution at 50°C during the addition.

c. Flowsheet

Utilizing information gained from the studies described, a tentative flowsheet was prepared for the continuous dissolution of 2.5 percent uranium-Zircaloy-2 alloy using ammonium fluoride-hydrogen peroxide (see Table 12). The flowsheet involves dissolution without reflux, and replacement of vapor loss with water. Such a dissolution is more trouble-free than dissolutions performed under total reflux, the latter having higher dissolution rates but involving air sparging to prevent solid formation within the dissolver. The dissolver product is stabilized with aluminum nitrate and nitric acid. The amount of stabilizer solution necessary depends upon the quantity of undissolved fines present in the dissolver solution. The greater the quantity of fines present, the larger the volume of stabilizer solution utilized in dissolving the fines before the stabilizing process begins. An equally effective flowsheet would probably be realized using 5.1M ammonium fluoride-1M ammonium nitrate as the dissolving reagent.

Table 12

TENTATIVE FLOWSHEET FOR THE CONTINUOUS DISSOLUTION (WITHOUT REFLUX) OF 2.5 PERCENT URANIUM-ZIRCALOY-2 ALLOYS USING AMMONIUM FLUORIDE-HYDROGEN PEROXIDE

		Fuel Charge (mg/min)	Dissol. Reagent Stream(a)	Conden-sate(b)	Dissol. Product at 50°C	Stabilizer Solution at 50°C	Adjusted Feed
Rate	ml/min		2.6	1.6	2.6	1.1	3.7
Zr	M	(135)			0.57		0.40
U	g/l	(3.5)			1.35		0.95
NH_4^+	M		5.1	3.7	2.8		2.0
H^+	M					2.3	0.68
H_2O_2	M		0.065		<0.005		<0.005
F^-	M		5.1		5.1		3.6
NO_3^-	M					9.2	2.7
Sn	M	(2.1)			0.006		0.004
Al	M					2.3	0.68

(a) Vapor loss is replaced by addition of water in a second stream at a rate of 1.6 ml/min.
(b) Hydrogen off-gas evolution, 66 cc/min.

3. Zirflex Solution Densities, E. M. Vander Wall, Problem Leader; J. L. Teague

An investigation of the densities of Zirflex process solutions is underway; determinations will be made at NH_4F concentrations ranging from 0.0M to 6.0M and NH_4NO_3 concentrations from 0.0M to 1.0M. The densities will also be determined for 0.1M and 0.5M $(NH_4)_2ZrF_6$ with added amounts of NH_4F.

To date measurements have been made on two different sets of solutions:

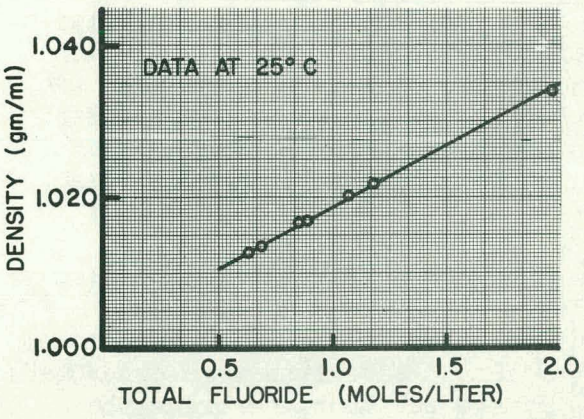

Fig. 3 - Density of 0.1M $(NH_4)_2ZrF_6$ Solution as a Function of Total Fluoride (at 25°C)

(1) 0.1M $(NH_4)_2ZrF_6$ to which has been added increments of NH_4F, until solubility limits are reached. Figure 3 shows the density values obtained for these solutions.

(2) 0.1M and 0.24M NH_4F containing 0.1M, 0.25M, 0.50M and 1.0M NH_4NO_3. The density values for these solutions are shown in Figure 4.

Values have been obtained by use of Weld's precision weighing bottles. The reference volume of these bottles is checked after each unknown sample by determining the weight of distilled water it will hold under the experimental conditions. This compensates for any etching, and consequent volume change, that may occur. The weighing bottles (with sample or water) are equilibrated at 25.0 ± 0.03°C. Duplicate samples show a precision of ± 0.0002 g/ml.

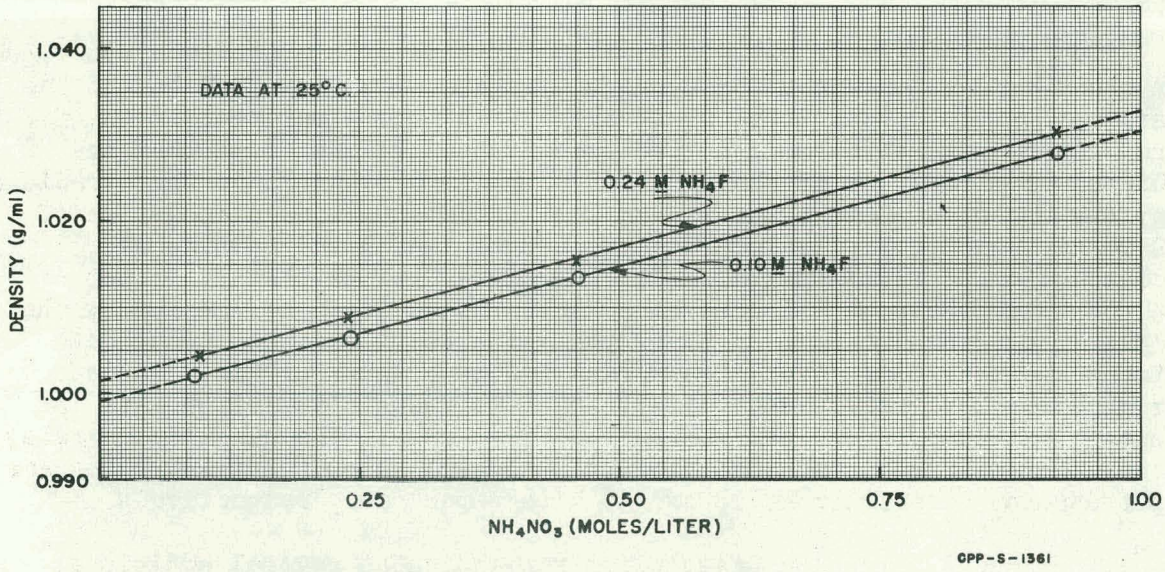

Fig. 4 - Density of NH_4F-NH_4NO_3 Solutions as a Function of Added NH_4NO_3 (at 25°C)

4. Continuous Dissolution Pilot Plant, J. A. Buckham, Problem Leader; H. V. Chamberlain, M. D. Martin, E. D. Howell and C. R. Ford

Initial testing of the zirconium dissolution pilot plant facilities was performed using aluminum dissolution flowsheets. After several modifications were made and equipment deficiencies were corrected, two preliminary runs were conducted using a 2 percent zirconium-98 percent uranium continuous flowsheet based on batch dissolution data. Several further deficiencies in equipment design were discovered during these two runs and are currently being corrected.

The aluminum dissolution flowsheet was chosen for initial testing because the technology of continuous aluminum dissolution is well known and it was believed that the equipment could be checked out more safely if hydrofluoric acid were not present. Five runs were conducted; the feed rate was varied from 5 to 60 liters per hour, covering the range for which the pilot plant was designed. On all runs, dissolution rates were as predicted from past experience. Several deficiencies, such as leaks in fittings and valves, were then corrected and a few minor modifications were made to provide for safer operation of the pilot plant.

The zirconium dissolution program was then started using 2 percent zirconium-98 percent uranium alloy. This fuel was selected for initial study since only small quantities of hydrofluoric acid are required and it is complexed with aluminum nitrate in the feed. Earlier corrosion studies showed that feed mixtures of nitric acid with complexed fluoride should be the least corrosive to Carpenter-20 equipment.

Two runs were made using a feed composition of 1M nitric acid, 0.30M hydrofluoric acid, and 0.35M aluminum nitrate. The fuel bed height was six feet in both runs. The feed rate was 18 liters per hour in the first run and 36 liters per hour in the second run. It was found that the dissolution rate was on the order of four times as great as that predicted by the use of scale-up factors for the laboratory batch dissolution of 2 percent zirconium-uranium fuel compared to batch and continuous dissolution of aluminum fuels. It therefore appears that it is not prudent to predict continuous dissolution rates for a new system by the comparison of batch data on this sytem with batch and continuous data for a known system. Preliminary data indicate that for the 2 percent zirconium-98 percent uranium fuel, the continuous dissolution rate is approximately proportional to the acid feed rate. The dissolution rates, based on a minimum number of product analyses, were 95 and 190 kilograms per day for feed rates of 18 and 36 liters per hour, respectively.

The second zirconium dissolution run indicated several additional equipment deficiencies and several modifications which would be necessary to insure safety of operation. During the early part of the second run, the canned rotor feed pump became inoperative and nitrogen pressure was used on the feed tank to obtain feed flow during the balance of the run. On subsequent examination of the pump it was found that erosion or corrosion of certain parts on the pump rotor had occurred and that deposits in this area had caused the rotor to freeze. An analysis of

the parts showed all the material to be Carpenter-20; at present the cause of the pump damage is not known. Since nitrogen pressure on the feed tank gives smooth feed flow control, since the repair of the pump may be costly, and since the exact causes of the erosion or corrosion are not known, it was decided to use nitrogen pressure in all subsequent runs. The feed preheater was found to have a leak between the tube side and the shell side and feed, mixing with the condensed steam, had corroded the iron steam traps and fittings on the condensate line. This leak may have been caused by stresses set up either when the vessel was annealed during fabrication or during actual operation. A new preheater of the shell and coil type is being fabricated to replace the old one.

Several cracks and leaks have occurred in and around the welds between wrought Carpenter-20 pipe and cast Carpenter-20 fittings. The majority of these leaks have been found adjacent to the welds in the cast material.

5. Evaporation and Mixing of Solutions in a Packed Vessel,
J. A. Buckham, Problem Leader; G. K. Cederberg

A study of the effect of packing on evaporation and air-sparge mixing of solutions in a vessel is being conducted to evaluate the feasibility of adding neutron-absorbing packing material to chemical processing equipment for criticality control purposes.

The feasibility of operating a 36-inch diameter ICPP batch evaporator, steam jacketed on the sides and bottom, when packed with Raschig rings or other suitable packing, is being studied. In the ICPP this evaporator is used for concentrating dilute solutions of enriched uranium which do not meet specifications. In an unpacked vessel very precise control of the total uranium content and the uranium concentration in the vessel must be maintained to prevent the occurrence of a nuclear criticality incident. Packing this evaporator with a chemically-inert, neutron-absorbing packing such as boron stainless steel Raschig rings, would greatly reduce the probability of a nuclear incident. An experimental program has been undertaken to determine satisfactory operating conditions using such a packing.

These experiments are being performed in a 30-inch diameter vessel jacketed on the side and bottom. Sixteen sample lines have been inserted into the vessel and are provided with gang-operated quick-opening valves to provide simultaneous samples at four elevations and three radial positions.

Concentration gradients in the vessel during evaporation, as well as rate of mixing of solutions by air-sparging, will be determined for the unpacked vessel and with the vessel packed with 1/2 inch and 1-1/2 Raschig rings. The extent of mixing is determined by analyzing simultaneous samples for copper (by a colorimetric method using a copper-EDTA complex) which is added as a concentrated nitrate solution, through the standard sparger distributor ring, at the start of each test.

A statistically-designed program is being followed to determine the effect of solution depth, solution density, solution viscosity, sparge air rate, and size of packing on mixing. Runs have been completed on the unpacked vessel; complete mixing is obtained in 1 to 3 minutes using air sparge rates of from 3 to 16 scfm. These studies are continuing.

IV. NEW WASTE TREATMENT METHODS

Section Chiefs: K. L. Rohde, Process Chemistry; D. W. Rhodes, Waste Treatment; J. I. Stevens, Waste Calciner Demonstration

The long range objective of many of the process developments at ICPP is improvement in nuclear waste management. Reduction in waste volumes produced in the reprocessing of fuel and more economic methods of waste handling and storage are specific objectives, which are stimulated by doubt as to the feasibility of indefinite tank storage of an ever-increasing quantity of liquid, and the belief that waste management is the major single economic factor in nuclear fuel processes.

Three routes to improved waste management are being pursued at ICPP. The reduction of liquid wastes to a solid form, effecting a substantial decrease in volume of material to be permanently stored, is exemplified by process development on the calcination of aluminum fuel wastes and laboratory studies on calcination of other type wastes. The development of headend processes which characteristically produce low volumes of waste is another approach to the problem; in the ARCO process, for example, the zirconium in a zirconium-bearing fuel is volatilized and separated as $ZrCl_4$ in the dissolution step. Zirconium may also be separated, together with fluoride, in a modified STR headend process by precipitation as barium fluozirconate. The third approach is directed to the separation of specific long-lived fission product from high-level wastes; e.g., the fission products from stainless steel fuels waste may be separated by a process involving mercury cathode electrolysis of the stainless steel components. Specific fission products may also be directly removed, as for example, the adsorption of cesium by ammonium phosphomolybdate.

In order to provide a basis for evaluation of possible headend and waste treatment processes, a review of the various aqueous processes for STR-type fuels with respect to the waste volume produced in each is presented in this report. The STR, modified STR, and Zirflex processes do not differ significantly in waste volumes. Headend treatment with barium, which makes it possible to remove zirconium and fluoride as insoluble barium fluozirconate, results in approximately a tenfold reduction in waste volume; this is one of the most promising of the developments presently under way. The ARCO process is also shown to give a quite low waste volume.

Polarographic curves on Cs-137, Ce-144 and Sr-90 in stainless steel wastes show that the Fe, Cr and Ni reduction by mercury cathode electrolysis can proceed without reduction of the three fission products down to 0.02M total ions. This would allow at least 98 percent removal of base alloy components from the waste.

The calcination of ZrF_4 wastes leads to large volumes of corrosive fluoride condensate. Addition of excess CaO to the waste prior to calcination, in an effort to retain the fluoride in a non-volatile form, was not completely successful. While quantitative precipitation of zirconium was obtained, the fluoride was not completely precipitated as calcium fluoride and calcination of the slurry would very probably release fluoride.

The solubility of ammonium phosphomolybdate in various mineral acids was measured for use in flowsheet studies for the removal of cesium from wastes. Solubilities range from 2.5 to >43 g/l at 25°C.

A. Waste Volume Comparison of Several Zirconium Processes, K. L. Rohde Problem Leader; O. W. Parrett and B. E. Paige

Several methods have been proposed for the aqueous processing of zirconium-uranium fuels of the STR or PWR core type. The first phase of the improvement of the STR process waste economics, through process chemistry, has involved reductions in the specific volume of extraction column raffinate and in the proportions of aluminum nitrate added for salting strength. The gains possible with such changes are limited and have probably been exhausted. Non-corrosive characteristics are obtained in the Zirflex process for enriched fuels at the expense of significantly increased waste volumes. The potential of the barium fluozirconate headend processes for reduction of waste volumes is very great but, while the results of the chemical flowsheet studies have been very favorable, the engineering aspects of the liquid-solid separation have not been demonstrated on a significant scale. In Table 13, comparison is made of these processes according to the quantities of radioactive waste producted.

The originally designed STR flowsheet[5] has been operated successfully on a production basis. The process currently in use[6] at the ICPP employs a more concentrated extraction feed, i.e., 0.67M zirconium instead of the 0.55M zirconium previously used, with the same aluminum nitrate salting strength used in both cases. This resulted in a 20 percent reduction in waste volume and the number of moles of aluminum used per fuel charge is reduced from 1395 to 1136.

Other modified STR flowsheets[7] have been verified on a laboratory scale. These methods utilize a reduced salting strength, 0.55M aluminum nitrate instead of the 0.75M previously used. This reduction offers increased stability and, therefore, greater uranium capacity is obtained with about a 25 percent raffinate volume reduction. The quantity of aluminum used is about 800 moles instead of the 1395 moles used with the originally designed flowsheet.

Details of the continuous dissolution work done with the Zirflex process are given in this report (Sec. III-B). The waste volumes produced by this method and the quantity of aluminum used are 28 percent greater than those experienced with the process as designed.

The barium fluozirconate headend precipitation methods[1][2][7][8][9] have also been verified on a laboratory scale. The novel feature in these flowsheets is the separation of the wastes into two levels of radioactivity. (See Table 13) The solid waste produced by the headend precipitation is expected to be only moderately radioactive.

Table 13

WASTE PRODUCTION COMPARISON OF PROCESSES FOR STR-TYPE FUELS

Each flowsheet is based upon the same fuel charge, 93 kg of zirconium alloy and 1.9 kg of uranium.

Process	Dissolver Reagent	Moderate Level Solid Waste (moles)	High Level Waste Solutions (liters)	High Level Waste (moles) Zr	Al
Original design STR flowsheet	10M HF	None	1946	1020	1395
Currently used STR flowsheet	10M HF	None	1515	1020	1136
Modified STR	10M HF	None	1460	1020	803
Zirflex	5.1M NH_4F	None	2500	1020	1704
Headend precipitation with $Ba(NO_3)_2$	12M HF	984 Zr	510	36	0
Headend precipitation with BaF_2 and $Ba(NO_3)_2$	7.4M HF	1005 Zr(a)	125	15	19
ARCO (with Pb recovery)	$PbCl_2$	1020 Zr(b) ~70 Pb	9	< 1	(Pb)~2

(a) Volume of dry solid estimated at 170 liters.
(b) Volume of dry $ZrCl_4$ = 170 liters based on a density of 1.4.

B. Mercury Cathode Electrolysis, R. L. Hickok, Problem Leader; K. T. Faler and D. R. Anderson

A polarographic study was initiated to investigate the electroreduction of fission product ions at the dropping mercury cathode. These data will be valuable in developing a waste treatment process to separate the alloy metal ions, iron, nickel and chromium from fission products in acidic, stainless steel waste solutions.

The initial results indicated that cesium, barium, strontium and yttrium in approximately 10^{-3}N acid solutions underwent electroreduction at the dropping mercury cathode above a potential that was characteristic for each ion. The rate of reduction of cerium increased gradually beginning at about -1.7 volts. The reduction mechanisms were shown to be independent of the concentration of fission product ions from tracer concentrations to about 1×10^{-3} molar, with cerium as the exception.

In solutions of typical waste concentration, the reduction of cesium, cerium and strontium was not detectable even with the use of radioactive tracers.

In general, the initial polarographic data indicated that transfer of the long-lived fission products cesium-137, cerium-144 and strontium-90 from the aqueous waste solution to the mercury cathode during electrolysis can be minimized by operating at voltages below approximately -2.0 volts vs the saturated calomel electrode and by maintaining the electrolyte concentration at approximately 0.02M or greater total ion concentration, thus permitting substantial separation of alloy metal from fission products.

Preliminary work on the properties of alloy metal-mercury cathode mixtures indicated that knowledge of viscosity will be important in handling of the cathode metal mixture. Exploratory tests indicated that it would be feasible to adapt a forced oscillation viscometer to the measurement of the viscosity of the alloy metal-mercury mixtures.

1. Experimental Methods and Equipment

Current-voltage curves for the fission product ions cesium, cerium, strontium, yttrium, and barium were obtained in neutral and in acidic solutions using the mercury drop-washing cell described in a previous report[1] and a Leeds and Northrup Type E Electro-Chemograph. A solution containing alloy metal ions in "polarographic concentrations" [5×10^{-4}M $Fe_2(SO_4)_3$, 1×10^{-3}M $NiSO_4$, 1×10^{-3}M $Cr_2(SO_4)_3$ and 5×10^{-4}M H_2SO_4] and a solution containing alloy metal ions in "typical waste concentration" [0.1M $Fe_2(SO_4)_3$, 0.01M $NiSO_4$, 0.02M $Cr_2(SO_4)$ and 0.5M H_2SO_4] were used to study the behavior of the fission products under an applied potential. The concentrations of the fission product ions varied from tracer level to as high as 0.1M, in which case the measured radioactivity of the fission products was plotted against applied potential. For intermediate concentrations, in the absence of alloy metal ions, the measured diffusion current was plotted against applied potential. Finally the effect of varying the total ion concentration of the solution on the electroreduction of the fission product ion was determined.

All voltages are reported as reduction voltages vs the saturated calomel electrode.

2. Results of Polarographic Studies

Current-voltage curves for the elements cesium, barium, strontium, yttrium and cerium are shown in Figures 5 through 10. The reduction of cesium, barium and strontium (Figures 5, 6 and 7) appeared to proceed in a straightforward manner. Reduction of these metals occurred at a characteristic voltage and was preceded by the reduction of hydrogen in acid solutions. The reduction of yttrium (Figure 8) resulted in two polarographic waves; a normal reduction wave, which represented the reduction of Y^{+3} to Y^{+2} starting at -1.75 volts, and a second wave beginning at -2.05 volts, which presumably represented the reduction of Y^{+2} to Y^{o}. The anomalous height and slope of the Y^{+2} to Y^{o} curve

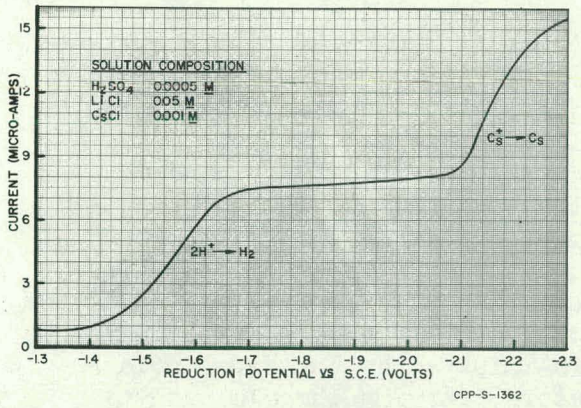

Fig. 5 - Polarographic Reduction of Cesium in Acid Solution at 25°C

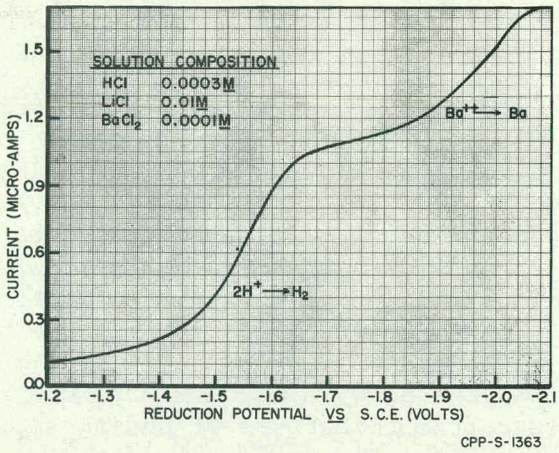

Fig. 6 - Polarographic Reduction of Barium in Acid Solution

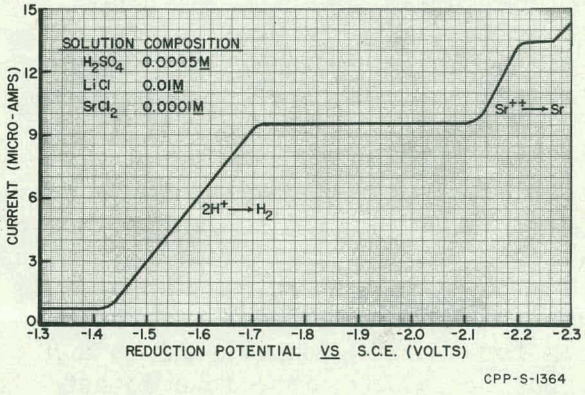

Fig. 7 - Polarographic Reduction of Strontium in Acid Solution

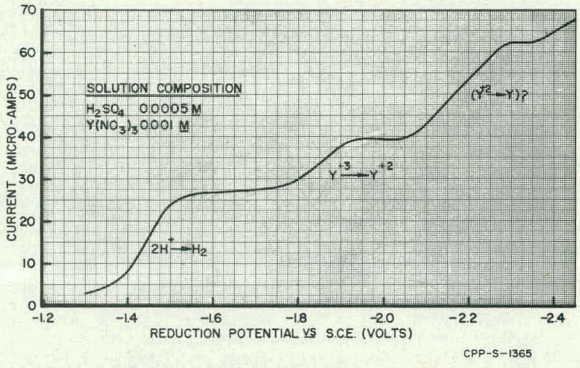

Fig. 8 - Polarographic Reduction of Yttrium in Acid Solution

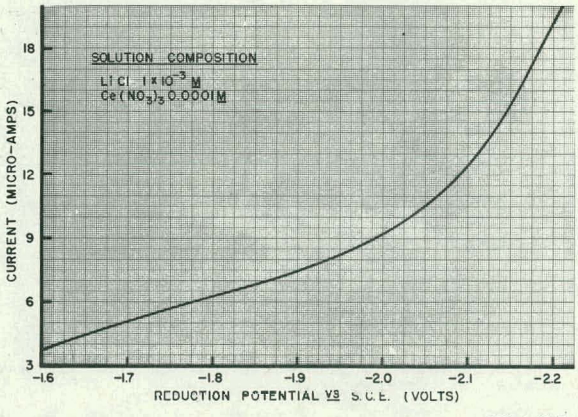

Fig. 9 - Polarographic Reduction of Cerium in Neutral Solution

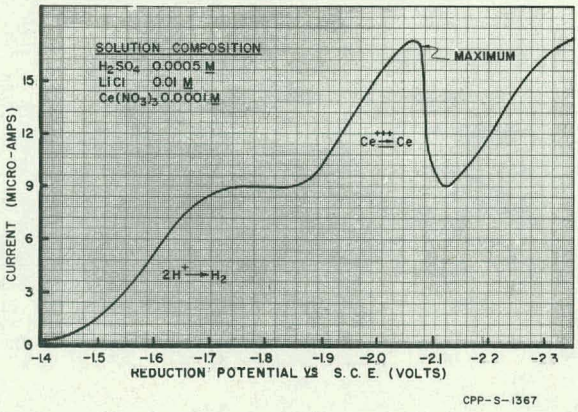

Fig. 10 - Polarographic Reduction of Cerium in Acid Solution

suggested that the reaction was more complicated than a simple electron transfer.

The behavior of cerium (Figures 9 and 10) differed markedly from that of the other ions. In neutral solution (Figure 9) a true polographic wave was never obtained, but instead a gradually rising current-voltage curve was observed, which indicated that reduction was occurring at a faster rate as the voltage increased. Hydrolysis of the cerium sulfate in neutral solution very likely was an important factor in producing this peculiar cerium curve. In acidic solutions (Figure 10) a polarographic wave began at about -2 volts (the predicted voltage half-wave potential for cerium), but the upper end of the curve was masked by a maximum that was not eliminated by the usual polarographic techniques of adding suppressors, varying the electrolyte content, etc.

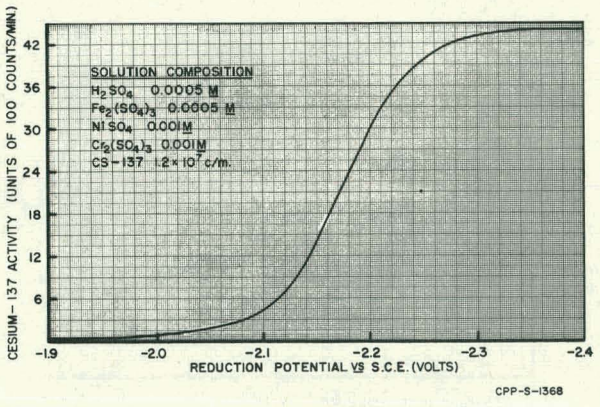

Fig. 11 - Polarographic Reduction of Cesium-137 in Acidic, Alloy Metal Ion Solution

Figures 11, 12 and 13 show the reduction of tracer concentrations of cesium-137, barium-137 and cerium-144, respectively in acid solutions at "polarographic concentrations" of iron, nickel and chromium ions. The curves for cesium and barium correspond very closely to the current-voltage curves for 1 x 10^{-3} molar concentrations of these ions (Figures 5 and 6), indicating that the reduction mechanism is the same for tracer concentrations as for "macro" concentrations and that the alloy metal ions do not affect the reaction mechanism. Cerium-144, on the other hand,

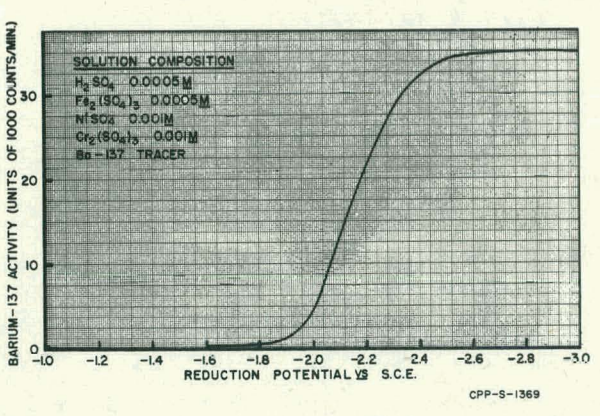

Fig. 12 - Polarographic Reduction of Barium-137 in Equilibrium with Cesium-137 in Acidic, Alloy Metal Ion Solution

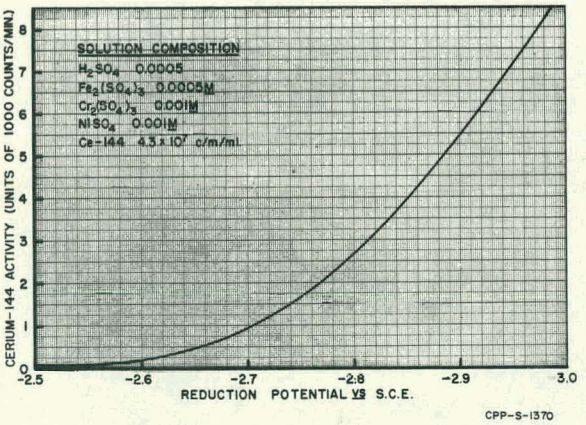

Fig. 13 - Polarographic Reduction of Cerium-144 in Acidic, Alloy Metal Ion Solution

produced a curve in acid solution similar to the curve obtained in neutral solution for cerium at concentration of 1 x 10^{-4}M. The reason for this anomalous behavior is not yet understood.

A study of the reduction of fission products at "typical waste concentrations" of alloy metals was limited to the range 0 to about -1.6 volts, which was below the half-wave potentials for the fission products. At more negative voltages the mercury dropping rate became erratic and mercury was partially retained at the aqueous-carbon tetrachloride interface so that accurate measurements were not possible. However, studies of the behavior of cesium and cerium during the reduction of iron, nickel and chromium through the voltage range 0 to -1.6 volts indicated no measurable quantity of either element was co-removed with the alloy metal ions.

The effect of varying the concentration of sulfuric acid, potassium sulfate and nickel sulfate on the reduction rate of cesium and cerium was studied at -2.3 volts for cesium and-2.8 volts for cerium. The effect of added ions was negligible up to about 0.02M total ion concentration. Above this concentration, the reduction rate of cesium and cerium decreased rapidly with increasing concentration of total ions.

3. Results of Mercury Recovery Studies

An investigation was initiated to study the viscosity, stability and methods of decomposition of the alloy-mercury mixture resulting from the mercury cathode electrolysis of stainless steel wastes. An electrolytic cell was constructed using a platinum mesh anode and a magnetically stirred mercury cathode. Iron, nickel or chromium in 0.5M sulfuric acid solution were electrolyzed into the mercury phase to provide a cathode of known composition.

Preliminary data indicated that a high iron-mercury phase was stable toward oxidation by air over a period of several days. The mixture separated into two phases on centrifugation, the lighter phase being identical in appearance but considerably more viscous than the heavy phase. Knowledge of the viscosity of the cathode mixtures was considered necessary to develop a waste treatment process. Preliminary attempts to measure viscosity of the mixtures indicated that viscosity measurements could be made in a forced oscillation capillary viscometer in which the amplitude of oscillation of the cathode material was compared simultaneously with the amplitude of oscillation of clean mercury as a standard. Work is continuing to adapt this method to the measurement of viscosity of cathode material as a function of alloy metal concentration.

C. Calcination of Zirconium Wastes, R. L. Hickok, Problem Leader; J. S. Madachy

Experimental work was initiated to study the chemistry of the calcination of waste solutions resulting from the aqueous processing of spent zirconium fuels, including precipitation prior to calcination to retain the fluoride in the calcined product. Preliminary results, using a waste solution containing all of the major chemical constituents

expected to be present in the zirconium type waste solutions, indicated that quantitative precipitation of zirconium was achieved by adding calcium oxide to the waste, but that quantitative precipitation of the fluoride was not obtained. Calcination of this slurry would very likely result in volatilization of the fluoride that was not precipitated as calcium fluoride.

Initial results of laboratory calcination of zirconium fluoride solutions, preliminary to the calcination of more complex solutions, indicated that complete conversion of zirconium fluoride to the oxide required about four hours in a batch type calcination. Additional experiments, using sand in the calciner, indicated that only a partial reaction of the sand with the fluoride, to form silicon tetrafluoride, occurred.

The preliminary results to date indicate that complete retention of the fluoride in the calcined solid may be difficult to achieve even with a pretreatment of the waste. The data also indicated that the laboratory calciner equipment must be modified and tested on simple solutions until successive experiments demonstrate that a reproducible material balance of the fluoride in the system can be obtained.

1. Precipitation of Zirconium

Experiments were performed to study the precipitation by calcium oxide of zirconium from synthetic zirconium process waste solutions as a pretreatment for calcination. The purpose of the pretreatment was to convert the fluoride in solution to calcium fluoride solid, which would prevent volatilization of the fluoride during calcination.

The synthetic waste composition was 0.45M zirconium, 0.67M aluminum, 0.97M hydrogen ion, 2.6M fluoride and 1.84M nitrate and was believed to contain all of the major chemical constituents which would be present in waste solutions resulting from the aqueous processing of zirconium fuels.

Solid calcium oxide was added to the synthetic waste solution, and the precipitate digested for several hours at below boiling temperatures. The filtered precipitate was then dried and ignited for various time intervals. The preliminary results indicated that zirconium was probably precipitated quantitatively. Apparently, also, a major fraction of the fluoride in a synthetic waste solution can be precipitated; however, the concentration of fluoride in the filtrates will have to be determined before the chemistry of the system can be well understood.

2. Equipment Operation and Development

A laboratory calciner, consisting of a closed stainless steel cylinder containing a platinum crucible as a calcination reaction chamber, was designed and fabricated. The calciner was constructed of 2-inch, schedule 40, stainless steel pipe, 6-inches long and was fitted with removable stainless steel plugs. A side arm from the calciner was connected to a copper absorption tube in which glass wool or similar

material could be inserted to react with any evolved hydrogen fluoride to convert it to silicon tetrafluoride. The absorption tube was connected to a scrubber containing 1.0N sodium hydroxide to trap the silicon tetrafluoride or hydrofluoric acid. A stream of hot air was drawn through the entire system during operation to sweep the gaseous reaction products through the collection system.

Five preliminary calcination runs were made using a zirconium fluoride solution containing 1.67M zirconium and 7.83M fluoride. In three of the experiments the zirconium fluoride solution was calcined in a bed of sand, and in the other two experiments only the zirconium fluoride solution was used. The calcination temperature was 500 to 525°C.

3. Results of Calcination Experiments

Evaluation of the preliminary calcination runs, based on a comparison of the weight of the residue in the crucible with the theoretical weight that would result from volatilization of the fluoride as silicon tetrafluoride and conversion of the zirconium to zirconium dioxide, suggests that the fluoride did not volatilize completely, or may have been volatilized as hydrogen fluoride rather than silicon tetrafluoride when sand was used in the calciner. The data also indicate that at least a four hour residence time in the calciner was necessary to convert zirconium fluoride to zirconium dioxide.

D. Removal of Long-Lived Fission Products from Waste Solutions, D. W. Rhodes, Problem Leader; M. W. Wilding

The removal of cesium and other long-lived radioisotopes from process waste solutions prior to calcination would simplify the requirements for off-gas cleaning in a calciner and reduce the requirements for storage of the calcined product. Laboratory experiments were performed to investigate factors affecting the adsorption by ammonium phosphomolybdate (APM) of cesium from process waste solutions.

The laboratory data indicated that the solubility of APM in mineral acids was in the order $HCl < HNO_3 < H_2SO_4 < HF$ and the range of measured solubility in 1N acid was 2.5 g/l to >43.0 g/l at 25°C. Solubility of the APM decreased by approximately an order of magnitude as the acidity decreased from 1.0N to 0.1N.

Distribution coefficients for cesium-137 were about 1×10^4 in nitric acid, aluminum nitrate or a mixture of both. The apparent distribution coefficient for cesium-137 increased by a factor of 1.6 as the concentration of aluminum nitrate decreased from 1.0M to 0.01M; however, sufficient data were not available to establish the reliability of this observation.

The data obtained during this report period demonstrated that APM, used as an inorganic ion exchange material, can remove essentially all of the cesium from acid solutions. The presence of about one molar aluminum nitrate, a serious competitor for the exchange sites on most

ion exchangers, had no inhibiting effect on the exchange reaction with APM. The solubility of solid APM in mineral acid solutions was low enough to be tolerated with the exception of solutions containing appreciable amounts of free HF. However, most processes which use HF also use a chemical constituent to reduce the free HF concentration to a relatively low value. The principal problem in the use of APM for the removal of cesium from waste solutions at present appears to be the serious pressure drops resulting from use of the finely divided material in an ion exchange column. Studies are underway to investigate this problem.

1. Experimental Methods

Laboratory batch equilibrium experiments were performed to investigate factors affecting the adsorption by ammonium phosphomolybdate (APM) of cesium from process waste solutions. Radioactive phosphorus (phosphorus-32) was incorporated into the APM by dissolving the solid in ammonium hydroxide solution containing the phosphorus tracer and then precipitating the APM with nitric acid. Samples of the dried precipitate were added to various aqueous solutions and the concentration of phosphorus-32 in the equilibrium solution was taken as a measure of the solubility of APM in that particular solution.

2. Experimental Results

The solubility of APM in solutions of various mineral acids is reported in Table 14.

Table 14

SOLUBILITY OF AMMONIUM PHOSPHOMOLYBDATE IN ACID SOLUTIONS AT 25°C

Acid	Concentration N	Solubility, grams/liter 24 Hr. Contact	120 Hr. Contact
Nitric	1.0	3.10	3.40
	0.1	0.36	0.58
	0.01	0.33	0.58
Sulfuric	1.0	6.80	7.20
	0.1	0.55	0.68
	0.01	0.49	0.62
Hydrofluoric	1.0	>43.00	>43.00
	0.1	3.60	4.60
	0.01	0.78	2.60
Hydrochloric	1.0	2.50	2.50
	0.1	0.75	0.52
	0.01	0.48	0.55

The data in Table 14 indicate that the solubility of APM in acid solutions was excessive only in the case of hydrofluoric acid at 1.0N acid or greater. In process waste solutions, the free hydrofluoric acid concentration probably would never approach 1.0N because of the necessity for complexing the fluoride prior to chemical processing of the dissolver solution. There was a marked difference in the solubility of APM in all of the acids at 1.0 and 0.1N acid indicating that any modification of the process waste that would decrease the acidity below 1.0N acid would be beneficial for the adsorption of cesium.

The results of equilibrium batch experiments to determine the effect on cesium adsorption of varying the concentration of aluminum nitrate and nitric acid are given in Table 15.

Table 15

EFFECT OF NITRIC ACID AND ALUMINUM NITRATE ON THE ADSORPTION BY AMMONIUM PHOSPHOMOLYBDATE OF CESIUM AT 25°C

Material	Concentration, M	Distribution Coefficient, K_d (Units of 10^4)
Aluminum Nitrate	1.0	1.71
	0.1	2.27
	0.01	2.87
Nitric Acid	1.0	1.96
	0.1	3.69
	0.01	1.68
	0.001	1.99
	0.0001	1.77
Nitric Acid (1N) and Aluminum Nitrate (variable)	1.0	1.05
	0.1	1.34
	0.01	1.65

The data in Table 15 suggest an increasing affinity of the APM for cesium with decreasing concentration of aluminum nitrate; however, sufficient data were not available to determine whether or not the trends were valid, and the only firm conclusion that can be drawn from the data at present is that adsorption of cesium was high through the range of the concentrations of aluminum nitrate and nitric acid that were investigated.

The extremely small crystal size of the ammonium phosphomolybdate resulted in very low flow rates when the solid was used in a packed bed, even with filler materials such as asbestos or vermiculite. An attempt was made, therefore, to use the solid in a fluidized bed with stainless steel filters at either end to contain the solid. Preliminary tests indicate that adequate flow rates could be obtained with this system. Additional experiments to measure the efficiency of the fluidized bed system for adsorbing cesium are planned.

E. Waste Calciner Demonstration

The progress of the research, development and demonstration work on waste disposal by calcination is the subject of a separate report[22]. An abstract, only, of the salient features of this work for the current period is presented here.

1. Laboratory Developmental Program, J. A. Buckham

The two-foot calciner was operated during this period to determine the ranges of the operating variables. Few operating difficulties were encountered, and a run of sixteen days duration yielded data indicating steady-state operation for the first time. Heat transfer data showed that overall heat transfer coefficients (from NaK to bed) ranged from 35 to 150 BTU/(hr)(ft^2)($^\circ$F).

A new twelve-inch diameter calciner, incorporating provisions for more versatile operation and control, is being constructed. Design of an apparatus for high-temperature, post calcination treatment has been started. A capacitance measuring device for remote determination of calcine bulk density and solids flow rate is being developed.

Initial testing of a particle coating apparatus has begun. Batch leaching has been studied and the possibility of leaching strontium and cesium from calcined alumina wastes, in a continuous countercurrent contactor, is being investigated.

2. Demonstration Facility, J. I. Stevens

The Waste Calciner Demonstration Facility was estimated to be approximately 88 percent complete at the end of the reporting period. ICPP first cycle extraction waste tanks were sampled and radiochemical analyses are in progress. One tank was sampled at various levels and the analyses indicate a high degree of chemical homogeneity. Heat generation rates in a 300,000 gallon waste storage tank were calculated from time-temperature curves and found to fall between the limits of 1.27 ± 0.37 BTU/(hr)(gallon).

V. GENERAL TECHNICAL SUPPORT

Section Chief: H. T. Hahn, Chemical Research

A. A Test of the Mixed-Electrolyte Conductance Theory, E. M. Vander Wall, Problem Leader; D. P. Pearson

The use of electrolytic conductance represents an important tool in defining the quantitative relationships between species existent in process solutions. These relationships have significance in application to both process problems and instrumental control. In order to analyze electrical conductance data for solutions of hydrolyzable metal salts, correction must be made for the conductance of the acid produced by hydrolysis.

When there exist more than two kinds of ions in solution, the mobilities of all ions present are altered, according to the theory of Onsager and Fuoss.[10] In a mixture of two 1 : 1 electrolytes, the change in equivalent conductance of the mixture relative to the arithmetic mean of the conductances of single solutions of the constituent electrolytes at the same ionic strength can be expressed as follows:

$$\Delta\Lambda \equiv \Lambda_{obs} - \frac{1}{\mu}\sum_i c_i \lambda_i = \frac{\alpha^* \Lambda^\circ \sqrt{\mu}}{\sum_i c_i \lambda_i} \sum_i c_i \lambda_i (Q_s' - 1) \qquad (1)$$

$$\frac{\sum c_i \lambda_i (Q_i' - 1)}{\sum c_i \lambda_i} \equiv Q_s' - 1 \qquad (2)$$

where $\Delta\Lambda$ is the change in equivalent conductance due to the mixture effect; Λ_{obs} is the observed equivalent conductance of the mixture; c_i is the concentration of the i th electrolyte and λ_i is its equivalent conductance at the ionic strength (μ) of the mixture; Λ° is the limiting equivalent conductance of the mixture; α^* is the relaxation coefficient in the Debye-Huckel-Onsager limiting law; and Q_i is the "mixture effect" coefficient of the i th ion which is calculable from the theory. In effect, the Q_s' expresses the change in the limiting law due to the mixture effect.

Without considering extended terms in the conductance equation, the application of equation (1) is restricted to ionic strengths not greatly exceeding 0.01M. The relative change in conductance should be greatest when there exist ions of the same sign with greatly differing mobilities, such as in a mixture containing hydrogen ions and cations of normal mobility. To test the theory, a few measurements of hydrochloric acid-potassium chloride mixtures have been made. These are shown in Figure 14.

Single electrolyte solutions were prepared from de-ionized, distilled water and reagent grade hydrochloric acid or fused, recrystallized potassium chloride. Concentrations were determined from conductance using the equation of Lind, Zwolenik and Fuoss[11] and the data of Owen and Sweeton[12]. All solutions were 0.01 ± 0.001M. Mixtures were prepared by weight within 0.01 percent from the single solutions. Resistance measurements were made with a Leeds and Northrup-Jones bridge at 25 ± 0.0002°C.

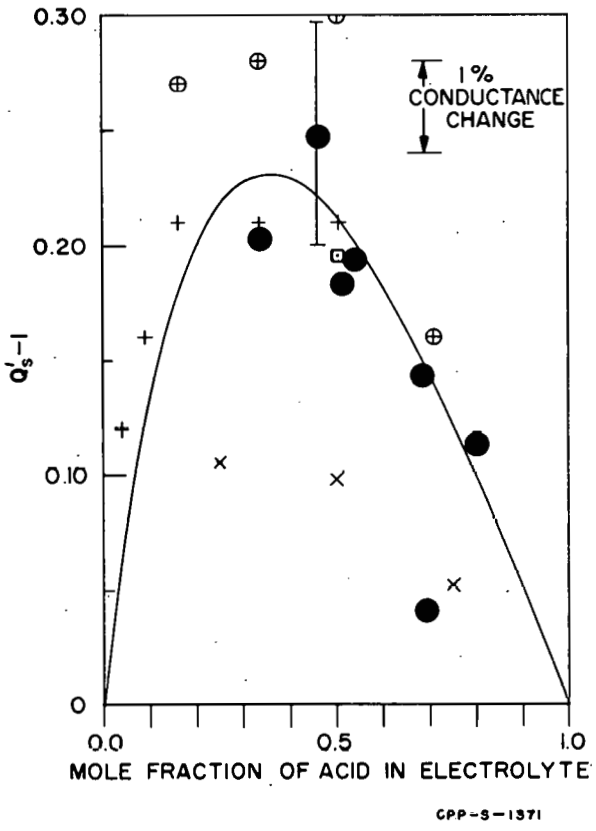

Fig. 14 - Mixed Electrolyte Relaxation Effect Coefficient for HCl-KCl Mixtures in Water as a Function of Electrolyte Composition

● HCl-KCl, μ = 0.01, (this work) (vertical line indicates known experimental uncertainty in one data point)
⊕ HCl-NaCl, $\mu \leq 0.02$, ref. (13)
\+ HCl-NaCl, $\mu > 0.02$, ref. (13)
X HCl-KCl, μ = 0.01, ref. (15)
□ HCl-KCl, μ = 0.01, ref. (14)

A number of investigators have studied the mixture effect previously; of these, three used HCl-KCl or HCl-NaCl mixtures.(13)(14)(15) The agreement between the three is not good, as may be seen from Figure 14 in which the solid line is calculated from theory. Only Bray and Hunt(13) investigated solutions of ionic strength less than 0.1M. Of the investigations of mixtures of two alkali chlorides, only two were made at ionic strengths of 0.01M or less.(16)(17) These both indicate that the change in conductance due to the "mixture effect" is only 45-65 percent as great as predicted by theory, although, in these cases, the absolute value of the discrepancy is not large because of the similar mobilities of the cations.

With the exception of the lowest point--which may be presumed to be in error-- the limited data reported here tend to confirm the theory for acid-salt mixtures.

VI. ELECTROLYTIC DISSOLUTION SYSTEMS

Section Chiefs: K. L. Rohde, Process Chemistry; H. T. Hahn
Chemical Research

With the advent of many new fuel compositions, it has become increasingly difficult to apply to them the dissolution chemistry of existing processes. Need for a universal headend process is continually becoming more acute. Scoping studies at the ICPP have shown the electrolytic dissolution method to come as close to handling all fuels as any single method. The electrical potential overcomes the passivity of stainless steel in nitric acid solutions. Zirconium metal shows partial solubility and partial hydrolysis to solid hydrates in aqueous sytems. This latter problem may be avoided by electrolysis in non-aqueous HCl-methanol, a system which opens an entirely new technology in fuel recovery. In aqueous systems with UO_2 clad in a metal, it may be possible to declad the UO_2 since the metal can be dissolved electrochemically and the oxide by chemical means.

The aqueous electrolytic studies in nitric acid have been extended to chemical flowsheet design. The particles of stainless steel which fall undissolved from the anode matrix during an electrolytic dissolution could represent a substantial dissolver design or solution clarification problem. In a statistically designed (2^3) dissolution experiment at 40 and 90°C, 0.4 and 1.2 amp/cm^2 anode current density and 1 and 5M hydrogen ion in the dissolver solution, it was found that the lower temperature always was associated with lower sludge production as was high current density-high acidity and low current density-low acidity. The stoichiometry was 1.33 and 1.45 moles of nitric acid consumed per equivalent of metal dissolved at 1 and 5M hydrogen ion, respectively. Potential-current data show that stirring gives a limiting current density 2.5 times the value obtained without stirring.

In order to apply electrolytic methods to decladding, a study was made of the rate of dissolution of uranium dioxide in order to locate a region where electrolytic decladding would be fast and chemical attack on uranium dioxide slow. Earlier data on the dissolution of uranium dioxide at temperatures between 25 and 100°C and at acidities between 0.3 and 2.0M nitric acid suggested a very strong temperature dependency for the uranium dioxide dissolution rate. Portions of uranium dioxide (342 mg of 70-100 mesh) were shaken with synthetic dissolver product solution for 10 and 30 minutes at 0, 13 and 25°C. With uranium losses to the solution as low as 0.3-0.4 percent for 10 minutes contact time at 13°C, it would appear that a headend separation based on this principle might be practical.

A. Electrolytic Dissolution of Stainless Steel in Nitric Acid

1. Flowsheet Studies, K. L. Rohde, Problem Leader; C. E. May

Previous studies of electrolytic dissolution of several types of stainless steel have shown no systematic variation of the anode sludge

yield as a function of the cell operating conditions or the dissolver solution composition. The total cell potentials observed have shown only qualitative evidence of concentration polarization at 1.5 amp/cm^2 current density (Ref. (1), Sec. V-A). A further series of experiments was designed to explore, primarily, the possibility of minimizing the quantity of anode sludge, and secondarily, to note the variations in cell potential and dissolution stoichiometry.

a. Experimental Conditions

A cylindrical cell utilizing nominal one-quarter inch, 304 stainless steel rods for anodes, and the interior surface of a nominal three-quarter inch stainless pipe for a cathode, was assembled in a solution circuit which included the cell, a vented condenser, a reservoir-heat exchanger, rotameter and pump. The dissolver solution was cirulated downward through the cell at a rate of 1.8 g/(cm^2)(sec). Reynolds numbers were about 500 and 300 at 90°C and 40°C, respectively, indicating non-turbulent solution flows. Forced circulation eliminated the variations in agitation caused by convection currents which were experienced previously, which were caused by convection currents. Anodes were changed regularly during the experiments so that actual current densities of 1.2 to 1.6 and 0.39 to 0.55 amp/cm^2 were experienced on the anode at the nominal values of 1.2 and 0.4 amp/cm^2. The cathode current densities were 0.36 and 0.12 amps/cm^2, respectively. As before (Ref. (1), Sec. V-A), the experiments were initiated in dissolver product solutions of approximately steady state composition, with sampling and reagent addition carried out to maintain the composition at the steady state values throughout the run. The anode sludge from the dissolver accumulated in the reservoir and was recovered from the dissolver solution, dried and weighed after the dissolution of approximately 21 grams of steel.

b. Results

The experimental conditions and observations are given in Table 16. Experiments 1 through 8 made up a complete survey of two levels of the variables, current density, dissolver product solution acidity and operating temperature. Experiment 9 was a duplicate of 7, and the others were run to supplement the data from the designed experiment.

Anode Sludge

The approximately 10 micron diameter particles of stainless steel which fall undissolved from the stainless steel anode matrix during an electrolytic dissolution could represent a substantial dissolver design or solution clarification problem. The statistical analysis of the results of experiments 1 through 8 of Table 16 showed that the effects of temperature and the current density-hydrogen ion interaction were significant at the 0.01 significance level. The lower temperature consistently produced less sludge. High current density-high acidity and low current density-low acidity also favored minimum sludge as shown in Figure 15. Experiment 10 indicates that the nitrate ion, perhaps as a measure of ionic strength, gave a better correlation than hydrogen ion with the amount of anode sludge produced.

Table 16

ELECTROLYTIC DISSOLUTION OF TYPE 304 STAINLESS STEEL IN NITRIC ACID
CONTROL OF ANODE SLUDGE

Exp.	Conditions: Current Density amp/cm²	Conditions: Temp. °C	Dissolver Product Composition: H^+ M	Dissolver Product Composition: S.S. Metals g/l	Dissolver Product Composition: NO_3^- M	Observations: Anode Sludge g/100g	Observations: Cell Potential V	Observations: Stoichiometry moles acid / moles metal
1	1.2	90	1	71	4.6	1.92	2.9	1.38
2	0.4	90	1	71	4.6	1.40	1.9	1.38
3	1.2	40	1	71	4.6	1.14	3.5	1.26
4	0.4	40	1	71	4.6	0.48	2.3	1.37
5	1.2	90	5	71	8.6	1.80	2.7	1.51
6	0.4	90	5	71	8.6	3.66	1.8	1.46
7	1.2	40	5	71	8.6	0.20	3.3	1.49
8	0.4	40	5	71	8.6	2.6	2.0	----
9	1.2	40	5	71	8.6	0.32	3.0	1.34
10	1.2	40	2	129	8.6	0.30	5.1	1.34
11	1.2	40	2	71	5.6	0.76	3.1	1.24

Cell Potential

The cell potentials were observed, incidentally, in these constant current experiments. As before, the variation during the experiment was only a few tenths volt. The results of experiments 1 through 8 were analyzed for the effect of variation in hydrogen ion and temperature on the cell potential at high and low current densities, separately, and the values for both current densities combined.

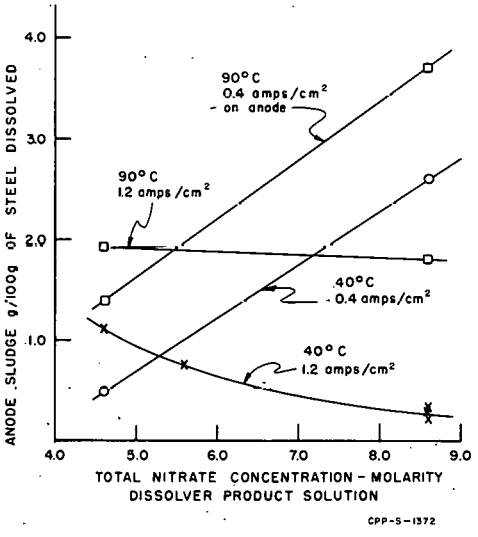

Fig. 15 - Anode Sludge Formation in Electrolytic Dissolution--Type 304 S.S. dissolving in nitric acid with stainless steel metal nitrate present

At the higher current density, 1.2 amp/cm², the effect of temperature was significant at the 0.08 significance level and the effect of hydrogen ion at the 0.15 significance level. At low current densities neither effect was significant at less than the 0.2 significance level. The combined data showed the effects of temperature and acid as significant at the 0.16 and 0.2 significance level, respectively.

Thus, at high current densities only, there was some evidence of concentration polarization as shown by the effect of hydrogen ion (which is not here independent of the nitrate ion). The mechanical agitation, equivalent to a solution velocity of about 1.8 g/(cm^2)(sec), was inadequate to prevent this effect.

Chemical Stoichiometry

The mean values of the acid consumption per mole of metal dissolved at each of the two levels of the variables, current density, temperature, nitrate ion and hydrogen ion were examined for significant difference. The significance levels in the "t" test were $\gg 0.1$, >0.1, >0.1 and 0.03 respectively. This is regarded as firm evidence that the stoichiometry does not vary with current density between 0.36 and 0.12 amp/cm^2 on the cathode, and that variation with temperature is unlikely between 40 and 90°C. The variation of stoichiometry with the hydrogen ion concentration of the dissolver solution appears to be significant and more pronounced than the relationship between the stoichiometry and the total nitrate concentration. The two variables of nitrate and hydrogen ion were so closely associated in the design of the experiment that their effects are not clearly separated by these results and analysis. The best stoichiometry values are 1.33 and 1.45 moles of nitric acid consumed per equivalent of metal in the dissolver product at 1 and 5M hydrogen ion and 4.6 and 8.6M nitrate, respectively. This corresponds to a calculated off-gas primarily of nitric oxide or mixtures of nitric oxide and nitrogen dioxide. Ammonium analyses of the dissolver products showed less than 0.015 equivalents of ammonium ion produced per equivalent of stainless steel dissolved. Nitrous acid, if produced as a reduction product, would be titrated as acid in the analytical method used, yielding a stoichiometry of 1.00 since no hydrogen ion would be lost in the reaction. It is concluded that neither ammonium ion nor nitrous acid are important final products of the nitric acid reduction under the operating and chemical conditions tested here.

2. Headend Separation of Clad from Uranium Dioxide Cores,
K. L. Rohde, Problem Leader; C. E. May

One of the more interesting general aspects of the electrolytic dissolution process for stainless steel clad uranium dioxide fuels, such as APPR, is that the stainless steel dissolution proceeds by an electrochemical process and the uranium oxide dissolution by a chemical process. Although the electrochemical process is not totally independent of the chemical parameters, it was felt that possibly sufficient difference in the relative dissolution of the two components could be brought about by adjustment of acidity and temperature in the dissolver to produce a usable headend separation of the uranium and cladding material.

Earlier data on the dissolution of uranium dioxide at temperatures between 25 and 100°C, and at acidities between 0.3 and 2.0M, suggested a very strong temperature dependency for the uranium dioxide dissolution rate (Ref. (1), Sec. V-A). The current data extending down to 0°C and to 0.2M nitric acid verify this dependency and seem to indicate an acceptably low order of uranium loss to the decladding waste.

a. Experimental Conditions

Portions of uranium dioxide (342 mg of 70-100 mesh) were shaken with synthetic dissolver product solution in flowsheet proportions for 10 and 30 minute periods at 0, 13 and 25°C. The solution contained approximately 69 g/l of iron, chromium and nickel as nitrates in 18-8 stainless steel proportions. After contacting, the supernate was analyzed for uranium, with results as described in Table 17.

Table 17

DISSOLUTION OF URANIUM OXIDE AT LOW TEMPERATURES

342 mg of UO_2 shaken with 50 ml of electrolytic dissolver product solution (69g ss/l as nitrates)

Contact Time (min)	10		30	
Nitric Acid Conc. (M)	0.2	0.5	0.2	0.5
Temperature °C	Uranium Oxide Dissolved			
	%	%	%	%
0	0.2	0.25	0.75	0.51
13	0.33	0.38	1.6	3.3
25	2.0	1.9	5.0	8.1

b. Conclusions

With uranium losses as low as 0.3-0.4 percent for 10 minutes contact time at 13°C, it would appear that a headend separation based on this principle might be practical. As in most such flowsheets, a filtration or centrifugation is involved. In this particular case separation would be relatively simple; the presence of a small amount of supernate in the uranium stream would not be objectionable since only one anion, nitrate, is involved, and the salts will contribute to the total salting strength for uranium.

If other anions were involved the undissolved UO_2 would have to be washed free of the foreign anion, or the subsequent flowsheet designed to tolerate it. With only NO_3^- present, there is no need for washing the solid in the centrifuge; indeed the flowsheet provides for slurrying out the solid UO_2 in a small volume of the supernate.

3. Potential-Current Relationships, J. R. Aylward, Problem Leader

In support of the aqueous electrolytic dissolution program, the potential-current density curves for a type 304 stainless steel cathode were measured in a simulated dissolver solution containing 49 g/l of Fe^{+3}, 7.0 g/l of Ni^{+2}, 13 g/l of Cr^{+3}, 1N H^+ and 5N NO_3^-. Measurements were made with and without stirring at both 55°C and 80°C.

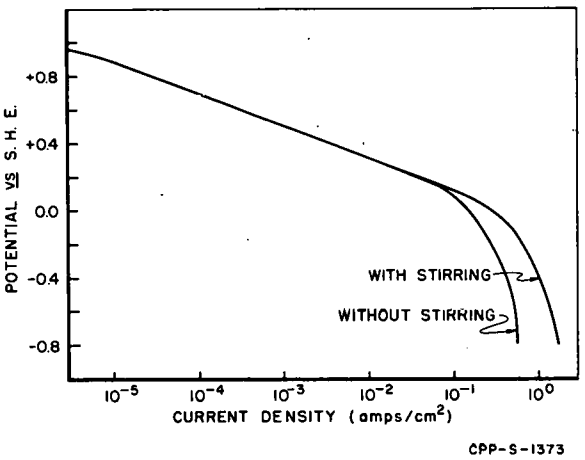

Fig. 16 - Potential--Current Density Curves for a Type 304 Stainless Steel Cathode in Simulated Nitrate Dissolver Solution at 80°C

The curves obtained, as shown in Figure 16, represent the average of at least two runs. Stirring increased the limiting current density by a factor of approximately 2.5, while temperature appeared to have little or no effect on the overall curve.

B. Electrolytic Dissolution in HCl-Methanol, J. R. Aylward, Problem Leader; E. M. Whitener

The investigation of a method suitable for separating uranium and zirconium in HCl-methanol dissolver solutions was continued. It has been determined that uranium(IV), as well as zirconium, would be precipitated by an alcoholic oxalic acid solution. However, uranium(VI) is not precipitated and all work has been carried out on uranium(VI) solutions. The oxidation of uranium(IV) to uranium(VI) was achieved by adding 30 weight percent of hydrogen peroxide to the HCl-methanol system. However, the presence of water, introduced by the addition of hydrogen peroxide, interferred with complete zirconium precipitation. The characteristics of the zirconium oxalate precipitated from various solution compositions are being studied.

The rate of the reaction of oxalic acid with the zirconium species in HCl-methanol solutions is being studied by potentiometric titration methods using a Ag, AgCl electrode and oxalic acid as the titrant. This method depends on the fact that the chloride bonded to the zirconium is displaced by the oxalate ion, causing an increase in the free chloride ion concentration in solution which is monitored as a potential change by the Ag, AgCl electrode. If this potential change is measured as a function of time, for a given amount of oxalate added, the reaction rate can be calculated. This procedure will also allow one to determine the average number of chlorine atoms per zirconium species in solution by observing the point at which the further addition of oxalic acid has no effect on the potential of the Ag, AgCl electrode.

VII. THE ARCO PROCESS--DISSOLUTION OF FUEL ALLOYS IN MOLTEN CHLORIDES

Section Chief: H. T. Hahn, Chemical Research

The ARCO process employs molten lead chloride as a dissolvent for zirconium-uranium alloys[18]. The product salt contains the uranium (principally uranium trichloride), together with excess lead chloride and the alkali, alkaline earth and rare earth fission products. Zirconium is removed during dissolution as the volatile zirconium tetrachloride. Lead chloride may be regenerated by dissolution in nitric acid and precipitation with hydrochloric acid. Certain nickel alloy container materials have demonstrated relatively good resistance to corrosion (3-8 mils/month) in the lead-lead chloride system.

Current research has been concerned with direct chlorination as an alternative to the previously proposed method of lead chloride regeneration. An extension of this to the ARCO process utilizes chlorination, by addition of Cl_2 to the lead chloride, and has been shown to dissolve, rapidly, stainless steel, chromium, niobium and many other metals used as fuel components. Work has continued in the areas of flowsheet definition, phase diagram studies and corrosion.

A. Chlorination of Lead, E. M. Vander Wall, Problem Leader; D. L. Bauer

The principal chemical cost of the ARCO process is that of lead chloride. It is possible to reconvert the lead resulting from the process into lead chloride by dissolution of the lead in nitric acid followed by metathesis with hydrochloric acid.[1] An alternative to this procedure is the direct chlorination of lead at temperatures greater than 500°C. Chlorination is advantageous since it is a one step process in which the lead chloride can be directly returned to the dissolver without intermediate aqueous purification steps. A logical extension is to rechlorinate the lead as it is formed in the dissolver, thus reducing the number of process vessels and material transfers to be made.

Several experiments were performed in conjunction with this direct chlorination of lead. The apparatus used was fabricated from Pyrex glass. The chlorine was initially passed through a glass coil which served as a pre-heater, then into a vertical tube which contained a sintered glass frit (medium porosity, 20 mm diameter). This served as a support for a column of molten lead as well as a means of dispersing the chlorine. Both the chlorine flow rate and the lead column height were varied in these experiments, the results of which are given in Table 18.

Two additional qualitative experiments were performed to obtain information on the rate of chlorination of lead using this technique. In one experiment a 30 mm glass frit and 5.6 mm thick lead layer were used and in the other a 20 mm glass frit and a 5.1 mm layer of molten lead. Since these layers are relatively thin, it was assumed, as an approximation, that the area of the lead surface which was to be chlorinated was equal to the area of the glass frit. On this basis, the

Table 18

CHLORINATION OF LEAD AT 520°C

(Diameter of lead column = 21.8 mm)

Chlorination Period (min.)	Lead Column Height (mm)	Cl_2 Flow Rate (g/min)	Pb Dissolved (g/min)	Cl_2 Utilization (percent)	Comments
15	4.2	0.033	0.072	76	
15	4.2	0.63	0.232	13	reached red heat
15	8.5	0.050	0.093	64	
20	10.3	0.20	0.37	64	
10	10.4	1.05	1.52	50	reached red heat
15	16.7	0.050	0.144	99	

chlorination rate using the 30 mm disc was 30 mg Pb/$(cm)^2$(min), while that using the 20 mm disc was 41 mg/$(cm)^2$(min). These rates are comparable to the average rates achieved over extended periods of time when lead is dissolved in nitric acid, 43 mg Pb/$(cm)^2$(min) for a 90 minute period[1].

It is evident from the data in Table 18 that both the chlorine flow rate and the thickness of the lead layer affect the overall dissolution rate. An adequate conversion rate can be achieved with relatively low chlorine flow rates. An excessive flow rate can cause an undesirable heating of the system; however, it appears feasible to utilize the chlorine completely on one pass, and allow the heat of reaction to maintain the temperature of the system, by choosing the proper thickness of the lead layer and a reasonable chlorine flow rate.

B. Direct Chlorination of Metals in Molten Lead Chloride,
E. M. Vander Wall, Problem Leader; D. L. Bauer

Attempts have been made to establish a dissolution system which can be used effectively for both zirconium and stainless steel nuclear fuels. One possible dissolution agent potentially capable of dissolving both types of fuel is chlorine. Previous work[19] indicated that type 347 stainless steel and zirconium react readily with chlorine at elevated temperatures; however, the reaction between chlorine and a zirconium-uranium alloy proceeded only at considerably higher temperatures and left appreciable residue.

In the ARCO process, the molten lead chloride reacts readily with zirconium-uranium and Zircaloy-uranium alloys at 500°C, but the reaction with 347 stainless steel is very slow, 0.0087 mg/$(cm)^2$(min).[2] To enhance the dissolution rate of 347 stainless steel, gaseous chlorine was bubbled through molten lead chloride at 530°C. This dissolution was very successful, achieving a rate of approximately 30 mg/$(cm)^2$(min),

probably as a result of solubilizing a passivating lead film on the stainless steel.

The apparatus used for these experiments was similar to that employed for the chlorination of molten lead. A glass coil served as preheater for the chlorine and a vertical tube with a 20 mm sintered glass frit was used to support the molten lead chloride. The amount of lead chloride used as the solvent in each run was 13.2 grams. Samples of several metals which are either possible cladding materials for nuclear fuels or potential construction materials for chemical processing equipment were tested. The data obtained are given in Table 19. The free energies of formation[20] at 800°K are also given; for comparison, the free energy of formation at 800°K for lead chloride is -29.0 kcal/gram atom of chlorine.

Table 19

RATES OF DISSOLUTION OF METALS IN Cl_2-$PbCl_2$ AT 530°C

Metal	Cl_2 Flow Rate	Dissolution Rate	Free Energy of Formation ($M + 1/2\ Cl_2 = MCl$) kcal/gram atom of Chlorine	
	mg/min	mg/(cm)^2(min)	Product	$\Delta F°_{800°K}$
Aluminum	33	12.0	$AlCl_3(g)$	-46.6
Aluminum	800	34		
Chromium	33	19	$CrCl_2(s)$	-35.2
			$CrCl_3(s)$	-29.7
Copper	33	8.67	$Cu_2Cl_2(l)$	-24.0
Gold	33	0.067	AuCl(s)	+ 1.8
Magnesium	33	15	$MgCl_2(s)$	-61.2
Molybdenum	33	0.097	$MoCl_5(g)$	- 8.4
Molybdenum	800	0.061		
Monel	33	0.193		
Monel	800	3.08		
Nickel	33	0.024	$NiCl_2(s)$	-22.1
Nickel	800	0.261		
Niobium	33	1.69	$NbCl_5(g)$	-12.8
Niobium	800	14.60		
Silver	33	0.533	AgCl(l)	-20.3
Silver	800	2.31		
347 Stainless Steel	33	4.37		
347 Stainless Steel	800	29.87		

The flow rate of 800 mg/min of chlorine was used to determine what one might expect as a maximum possible rate of dissolution of the metals at these temperatures. From the data, it is apparent that aluminum, chromium, copper, lead, magnesium, Monel, niobium and 347-stainless steel dissolve quite rapidly in these mixtures. Previous data have established that lead chloride alone dissolves zirconium and Zircaloy very rapidly. The rates reported for chromium and magnesium are based on the initial area and total weight, since the samples were completely dissolved. The sample of aluminum also dissolved completely when the high chlorine flow rate was used. Therefore, the rates reported in these instances are the lower limits of the dissolution rate.

The other metals tested dissolved too readily to serve as suitable container materials unless otherwise protected. However, a disc of Coors Type AD-99 Alumina Ceramic was immersed in molten lead chloride through which was passing 50 mg of chlorine per minute for five hours. The sample exhibited no apparent surface attack and gained 5 mg during this period. The weight gain may have been due to incomplete removal of lead chloride from the surface.

C. Flowsheet Aspects, H. T. Hahn

Replacement of the acid lead recovery steps by direct chlorination simplifies the flowsheet aspects of the ARCO process. The number of

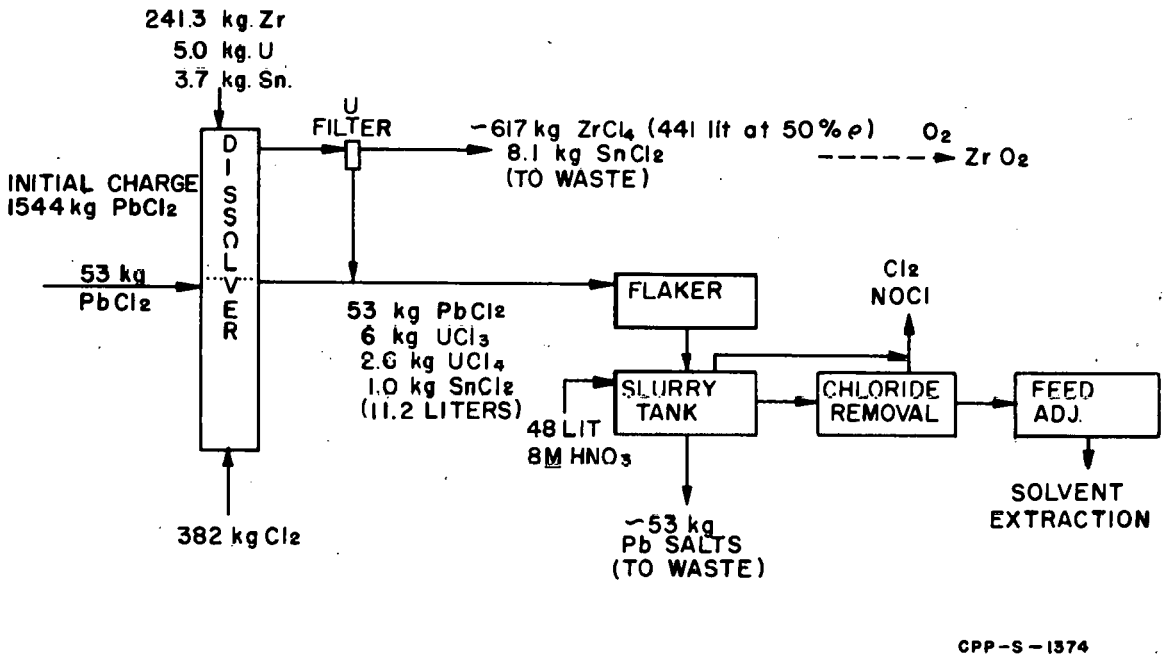

Fig. 17 - ARCO Process Flowsheet--5 kg/day plant with lead recovery by chlorination

operations and transfers, and the amount of equipment, are considerably reduced. Corrosion data for the chlorine-lead-lead chloride system are not yet available. However, there would seem to be no need for a separate lead chlorination unit unless the presence of a salt such as uranium chloride aggravates corrosion.

In situ chlorination in the dissolver would then require a balance of the chlorine and fuel feed rates. The lead chloride would function only as a means of heat and product removal. A chemical flowsheet based upon this concept, and designed to process a two percent uranium-zirconium alloy, is presented in Figure 17. Although corrosion may be anticipated to be greater with the presence of chlorine, modifications such as the controlled, localized admission of chlorine will be examined.

D. Corrosion in Molten Lead-Lead Chloride, N. D. Stolica, Problem Leader; G. S. Adams

Additional specimens of Hastelloy C, Inconel X and Incoloy 804 were immersed in molten lead and lead chloride for 18 days at 528°C. The procedure has been described previously[1]. The corrosion rates are given in Table 20.

Table 20

THE CORROSION OF SELECTED ALLOYS IN THE LEAD-LEAD CHLORIDE SYSTEM

(18 days, 528°C)

Alloy	Weld Status	Rate, Mils/Month
Inconel X	Unwelded	2.8 ± 0.0
Incoloy-804	Unwelded	9.3 ± 0.4
Incoloy-804	Welded	6.6 ± 0.7
Hastelloy C	Unwelded	7.8 ± 3.5

VIII. SMALL PLANT TECHNOLOGY

Section Chiefs: H. Schneider, Small Plant Projects; H. T. Hahn, Chemical Research

A study has been made of the technical and economic feasibility of a small scale reprocessing plant suitable for location at the Dresden reactor site and capable of handling the fuel load from the single reactor existing at that site.

The application of small plant technology to most of the fuels from civilian power reactors requires a knowledge of process chemistry under high fuel burnups. Irradiations of 10,000 to 30,000 MWD/ton are anticipated within the next few years and essentially no data exist on solvent stability or fission product behavior under these conditions. Although the problem is general to civilian power fuel processing, it will be necessary to obtain early data for application to the Dresden case of the small plant program.

Difficulties have been encountered at the ICPP in the processing of highly enriched uranium fuels of high burnup. These problems revolved around the fission product zirconium in the dissolver solution and its reactions with tributyl phosphate. This problem has been under investigation for over a year and is being broadened to include the civilian power fuels.

Present results on the TBP-HNO_3-Zr reaction in the organic phase show (1) that the zirconium-TBP reaction is first order with respect to zirconium, (2) the half time for the reaction increases as the zirconium concentration increases and (3) that the activation energy is 21.0 kcals. At 50°C the half time of the reaction is about 15 hours and of considerable process significance since it contributes substantially to TBP decomposition as compared with the nitric acid catalyzed decomposition.

A. Conceptual Design and Analysis of a Dresden Reprocessing Plant, H. Schneider, Problem Leader

A study has been made of the technical and economic feasibility of a small scale reprocessing plant suitable for location at the Dresden reactor site and capable of handling the fuel load from the single reactor existing at that site. A progress report on this project, which is published separately,[22] concludes that the installation and operation of such a plant is technically feasible, describes the design of a conceptual plant, assesses the associated hazards, presents cost data, and discusses development requirements.

The design of the plant is based on a concept originally developed by the Phillips Petroleum Company, AED, for application to remote package power reactors or foreign test reactors. Principal design considerations include: (a) limited extension of existing technology; (b) minimization of plant investment through compact design and maximum

use of existing reactor facilities; (c) minimization of manpower through extensive use of automatic controls; (d) emphasis on safety and minimization of hazards.

The actual process involves disassembly of fuel elements into individual fuel pins, by use of an underwater saw, followed by chopping of the pins to expose the uranium dioxide pellets. The pellets are then dissolved in nitric acid, leaving the cladding segments to be removed mechanically while the uranium and plutonium are decontaminated and partitioned in a Purex solvent extraction process.

The main process equipment is housed in a single, underground, concrete cell with groups of equipment being mounted, as functional units, so as to be separately removable by lifting sections of the top shield plug. Sampling, analytical, product preparation and waste handling facilities are provided.

Preliminary analysis of information presented supports the conclusion that sufficient safeguards can be incorporated into the reprocessing plant design to result in minimum hazard to site personnel and the general public, and to insure that operation of the power plant would not be jeopardized.

B. Process Development--Solvent Stability Studies, E. M. Vander Wall, Problem Leader; A. J. Moffat

The TBP-Zirconium Tetranitrate Reaction

The presence of zirconium in process solutions (from alloys, high burnup, or both) and its effect upon tributyl phosphate suggested that a better understanding of the tributyl phosphate-zirconium reactions would be desirable.

Extracted zirconium [$Zr(NO_3)_4 \cdot 2TBP$] (21) has been found to react with tributyl phosphate (TBP) to produce the relatively insoluble $Zr(NO_3)_2(DBP)_2$ by the following reaction: (1)

$$Zr(NO_3)_4 \cdot 2TBP \xrightarrow{TBP} Zr(NO_3)_2(DBP)_2 + 2C_4H_9ONO_2$$

This reaction is being studied for the purpose of determining rates, mechanisms and activation energy. As a continuation of this study, several experiments involving the TBP-zirconium reaction were completed at 50°C and one experiment was completed at 60°C. The conditions for these experiments are summarized in Table 21.

The reaction was followed by determining the rate of formation of n-butyl nitrate (by means of gas-liquid chromatography). (1) Initial zirconium and nitric acid concentrations in the organic phase were determined by titration of aliquots of the organic phase with sodium hydroxide, in the presence of and in the absence of sodium fluoride. (1)

Table 21

EXPERIMENTAL CONDITIONS FOR TBP-ZIRCONIUM REACTIONS

Zr(IV), M	HNO_3, M	Temp. °C	Refer to Figure
0.059	1.96	50	18
0.084	1.90	50	20
0.085	1.91	50	20
0.085	1.91	60	20
0.288	2.00	50	19

Figures 18, 19 and 20 depict the net rate of formation of n-butyl nitrate at three zirconium concentrations and two temperatures. In order to isolate the zirconium-TBP reaction from the HNO_3-TBP reaction, the experiments were followed for several days and the linear portion of the curve (e.g., from 3-20 days in Figure 18, due to the HNO_3-TBP reaction) was extrapolated back to zero time to determine the total amount of n-butyl nitrate produced by the zirconium-TBP reaction. This extrapolated n-butyl nitrate concentration (designated as $\underline{a}$) was then used to determine the ($\underline{a}$ - $\underline{x}$) values which are plotted in Figure 21. The n-butyl nitrate concentration at some time, $\underline{t}$, is designated as $\underline{x}$. The contribution of the acid reaction to $\underline{x}$ is within the experimental error.

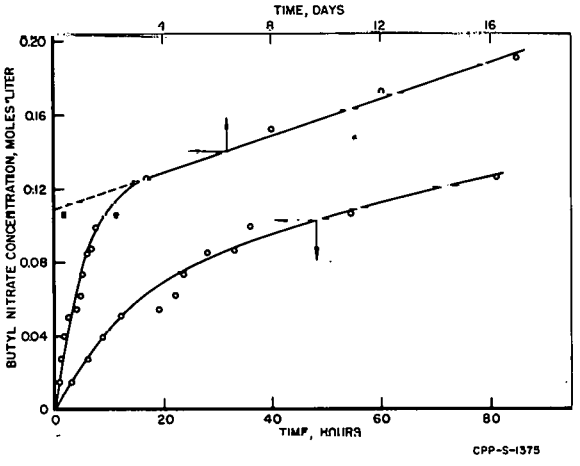

Fig. 18 - Formation of n-Butyl Nitrate--in 0.059M Zr-1.96M HNO_3, TBP solution at 50°C

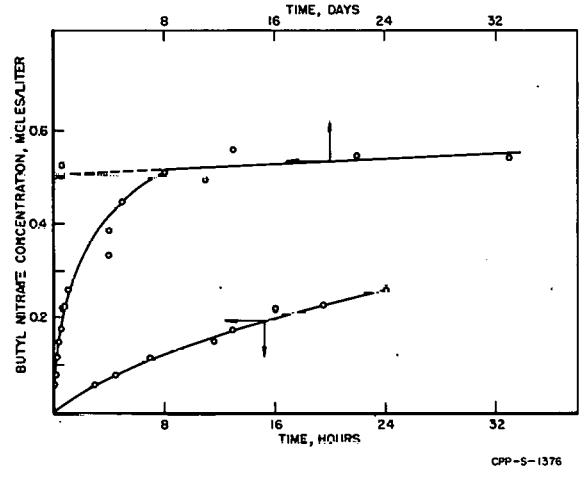

Fig. 19 - Formation of n-Butyl Nitrate--in 0.288M Zr-0.196M HNO_3, TBP solution at 50°C

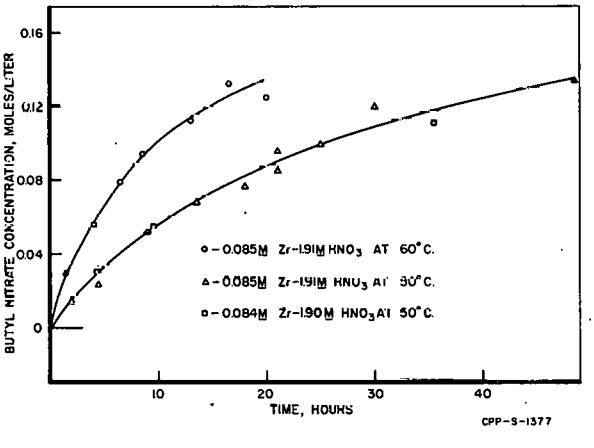

Fig. 20 - Formation of n-Butyl Nitrate--in 0.085M Zr-0.191M HNO_3, TBP solution.

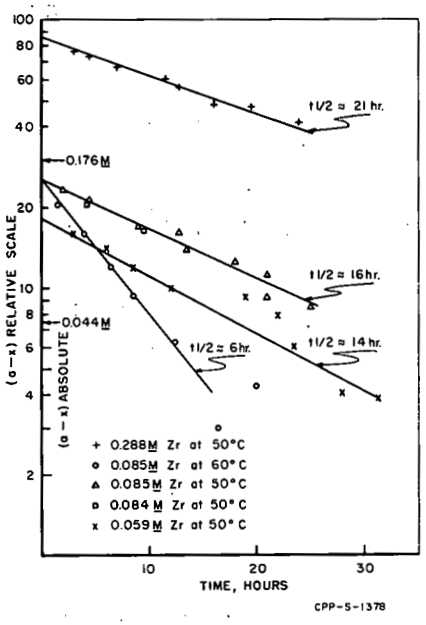

Fig. 21 - Plot Indicating First Order Relationship Between Initial Zirconium Concentration and Rate of Formation of n-Butyl Nitrate

Figure 21 indicates (a) that the zirconium-TBP reaction is first order with respect to the zirconium concentration and (b) that the time for one-half of the zirconium to react ($t_{1/2}$) increases as the zirconium concentration increases (see also Table 22). The data presented permit calculation of the activation energy for the reaction as approximately 21.0 kcal. The reason for the variation of $t_{1/2}$ with the zirconium concentration (Table 22) may be due to the decreased availability of TBP since, as the zirconium molarity is increased, more of the otherwise free or available TBP would be tied up in the $Zr(NO_3)_4 \cdot 2TBP$ complex.

Table 22

VARIATION OF $t_{1/2}$ WITH ZIRCONIUM CONCENTRATION AND TEMPERATURE

Zr M	$t_{1/2}$ (hrs)	Temp. °C
0.059	14	50
0.085	16	50
0.288	22	50
0.085	6	60

IX. REFERENCES

1. Bower, J. R., Idaho Chemical Processing Plant Technical Progress Report, October-December, 1959, IDO-14512

2. Stevenson, C. E., Technical Progress Report for July Through September, 1959, Idaho Chemical Processing Plant, IDO-14509

3. Moffat, A. J., Zirconium Fluoride Phase Studies, II. Sodium Fluozirconate Phase Relationships, IDO-14499, December 31, 1959

4. Gens, T. A., Modified Zirflex Process for Dissolution of 1-10 Percent U-Zr Alloy Fuels in Aqueous NH_4F-NH_4NO_3-H_2O_2: Laboratory Development, ORNL-2905, March 18, 1960

5. Classified Design Manual

6. Phillips Petroleum Co. Classified Report

7. Phillips Petroleum Co. Report in Preparation

8. Stevenson, C. E., Technical Progress Report for January Through March, 1959, Idaho Chemical Processing Plant, IDO-14471, August 27, 1959

9. Stevenson, C. E., Technical Progress Report for April Through June, 1959, Idaho Chemical Processing Plant, IDO-14494, March 22, 1960

10. Onsager, L. and R. M. Fuoss, J. Phys. Chem., 36, 2689 (1932)

11. Lind, J. E., J. J. Zwolenik and R. M. Fuoss, J. Am. Chem. Soc., 81, 1557 (1959)

12. Owen, B. B. and F. H. Sweeton, J. Am. Chem. Soc., 63, 2811 (1941)

13. Bray, W. C. and F. L. Hunt, J. Am. Chem. Soc., 33, 781 (1911)

14. Bennewitz, K., C. Wagner and K. Kuchler, Physik. Z, 30, 623, (1929)

15. Longsworth, L. G., J. Am. Chem. Soc., 52, 1897 (1930)

16. Krieger, K. A. and M. Kilpatrick, J. Am. Chem. Soc., 59, 1878 (1937)

17. Kell, G. S. and A. R. Gordon, J. Am. Chem. Soc., 81, 3207 (1959)

18. Hahn, H. T. and E. M. Vander Wall, Salt Phase Chlorination of Reactor Fuels. I. Dissolution of Zirconium Alloys in Lead Chloride, IDO-14478, (1959)

19. Householder, A. S., Mathematics Panel Quarterly Progress Report for the Period Ending October 31, 1951, ORNL-1141, February 8, 1952

20. Glassner, A., Thermochemical Properties of the Oxides, Fluorides and Chlorides to 2500°K, ANL-5750, 1957

21. Hudswell, F. and J. M. Hutcheon, Methods of Separation of Zirconium From Hafnium and Their Technological Implications, AERE Harwell (1955). U. N. Conference on Peaceful Uses of Atomic Energy (1955), Vol. 8, 563, paper p. 409

22. To be Reported

PHILLIPS
PETROLEUM
COMPANY

ATOMIC ENERGY DIVISION